to the instruction manual of the 5′ Rapid Amplification of cDNA Ends (RACE) System (Invitrogen), and sequencing was carried out using the ABI 310 autosequencer.

Knockdown of hamster and human *ORP5* using short interfering RNA. Complementary single-stranded short interfering RNA (siRNA) molecules were annealed into duplexes at a final concentration of 20 μmol/L. Duplex siRNA was used against hamster ORP5 (CCG CUG AAU GGG UCU GCU UTT/AAG CAG ACC CAU UCA GCG GTT), hamster control (CCG AGU AGG UGU CGC UCU UTT/AAG AGC GAC ACC UAC UCG GTT), human ORP5 (UUC GUG AGG UAA GGA CCU GGU UCU G/CAG AAC CAG GUC CUU ACC UCA CGA A), and human control (UCU UGU UCU CCU CUG ACA CUG UCU C/GAG ACA GUG UCA GAG GAG AAC AAG A). RNA inhibition was carried out according to the standard protocol using Lipofectamine 2000 (Invitrogen). The cells transfected with hamster ORP5 siRNA were designated PC1.0-ORP5, the cells transfected with hamster control siRNA were designated PC1.0-control, the cells transfected with human ORP5 siRNA were designated Capan2-ORP5, and the cells transfected with human control siRNA were designated Capan2-control.

Construction of the hamster and human *ORP5* expression vector, and stable transfection of *ORP5*. The primer sets for full-length *ORP5* amplification were as follows: hamster *ORP5*, 5′-ATG AAG GAG GAG GCC TTT CT-3′ (forward) and 5′-TTT GAG GAT ATA GTT AAT GAA TAG-3′ (reverse); and human *ORP5*, 5′-ATG AAG GAG GAG GCC TTC CT-3′ (forward) and 5′-TTT GAG GAT GTG GTT AAT GAA CA-3′ (reverse). The polymerase chain reaction products of hamster *ORP5* and human *ORP5* were cloned into the pcDNA3.1/V5-His TOPO vector (Invitrogen). The expression vectors for hamster and human *ORP5* were designated pcDNA/hamORP5 and pcDNA/huORP5, respectively. Also, the expression vector for *LacZ*, designated pcDNA/LacZ, was used as the control vector. For stable transfection, the cells were selected using 600 μg/mL G418 for 2 weeks and thereafter maintained in the presence of 300 μg/mL G418. PC1 transfected with pcDNA/hamORP5 was designated PC1 + ORP, and PC1 transfected with pcDNA/LacZ was designated PC1 + LacZ. Similarly, Hs700T transfected with pcDNA/huORP5 was designated Hs700T + ORP, and Hs700T transfected with pcDNA/LacZ was designated Hs700T + LacZ.

Detection of *ORP5* expression by reverse transcription–polymerase chain reaction and western blotting. Total RNA extraction of siRNA- or expression vector-transfected cells was carried out at 0, 24, 48, and 72 h after transfection using TRIzol along with DNase treatment. cDNA was synthesized using SuperScript III (Invitrogen), in accordance with the manufacturer's instructions. Reverse transcription–polymerase chain reaction (RT-PCR) was carried out under the following conditions: initial denaturation at 94°C for 3 min, followed by 27 cycles of amplification (denaturation at 94°C for 30 s, annealing at 56°C for 30 s, and extension at 72°C for 30 s), and terminal extension at 72°C for 3 min. The primers used for the RT-PCR amplification were as follows: hamster ORP5, 5′-TGA AGC TTG TGC TAC GAT GG-3′ (forward) and 5′-TGT TCT TCT CGC ATG CGA TG-3′ (reverse); human ORP5, 5′-CTT CTA CAA GAA GCC CAA GG-3′ (forward) and 5′-GAG ATC TGG TTG ATG CTG GT-3′ (reverse); and hamster and human glyceraldehyde-3-phosphate dehydrogenase (GAPDH), 5′-TGA CCA CAG TCC ATG CCA TC-3′ (forward) and 5′-CCA CCC TGT TGC TGT AGC C-3′ (reverse).

Protein extraction from the siRNA- or expression vector-transfected cells was carried out at 0, 24, 48, and 72 h after the transfection using cell lysis buffer (25 mmol/L Tris, 100 mmol/L NaCl, 2 mmol/L ethlenediamine tetra-acetic acid (EDTA), 1% Triton-X) containing protease inhibitor and phosphatase inhibitor. A total of 30 μg protein was loaded on to a 10% sodium dodecylsulfate–polyacrylamide gel electrophoresis gel and then transferred to a polyvinylidene difluoride (PVDF) membrane. The membrane was blocked with 5% skim milk (BD, Franklin Lakes, NJ, USA) in Tris-buffered saline (TBS)–Tween 20 (0.1%) at room temperature for 1 h and then incubated with polyclonal goat anti-ORP5 antibody (Imgenex, San Diego, CA, USA), β-actin antibody (Cell Signaling Technology, Beverly, MA, USA), or V5 antibody (Invitrogen) for 1 h at room temperature. The membrane was then rinsed twice for 10 min each with TBS–Tween 20 and incubated with antigoat secondary antibody (Santa Cruz Biotechnology, Santa Cruz, CA, USA) for 45 min at room temperature. The membrane was rinsed twice more for 10 min each with TBS–Tween 20 and once for 10 min with TBS, incubated with ECL-Plus (GE Healthcare, Buckinghamshire, UK), and then exposed to X-ray film and developed.

Invasion assay. To examine the invasiveness of the cell lines, we used a Matrigel invasion chamber (Becton Dickinson Labware, Bedford, MA, USA). The PC1.0-ORP5, PC1.0-control, Capan2-ORP5, and Capan2-control cells were plated 5×10^4 cells/well in a 24-well Matrigel invasion chamber in the presence of a chemoattractant. The cell counts of the invading cells were determined 22 h after seeding. Assays to determine the invasiveness of PC1 + ORP, PC1 + LacZ, Hs700T + ORP5, and Hs700T + LacZ cells were carried out in the same manner.

Human pancreatic cancer tissue samples. From 1982 to 2001, primary pancreatic cancer patients who underwent detailed pathological analyses and regular follow up at the Kumamoto University Hospital were recruited into this study. Patients who had metastasis at the time of the operation, did not have curative operation, or received preoperative treatment, such as chemotherapy or radiation therapy, were excluded from the study. Analysis for ORP5 expression by immunohistochemistry was carried out in a total of 56 specimens of pancreatic cancer. Based on the results of the pathological analyses, the cancers were classified according to the Japanese Classification System.[29] All patients provided written informed consent prior to participation in the study after receiving a thorough explanation of the purpose and method of the study, which was approved by the Institutional Review Board of Kumamoto University, Japan.

Immunohistochemical staining for ORP5. Paraffin-embedded tissue sections were deparaffinized in xylene, rehydrated in progressively decreasing concentrations of ethanol, and rinsed with ultrapure water. Antigen retrieval was carried out by boiling the tissue sections in 10 mmol/L sodium citrate buffer (pH = 6.0) at 121°C for 15 min in an autoclave. Thereafter, the slides were rinsed with ultrapure water and endogeneous peroxidase was blocked with a 3% hydrogen peroxide solution in 100% methanol for 30 min, followed by two rinses for 5 min each with phosphate-buffered saline (PBS). Non-specific protein binding was blocked with 5% skim milk in PBS for 30 min at room temperature. After draining off the skim milk solution, polyclonal goat anti-ORP5 antibody was added at a dilution of 1 : 50, followed by incubation overnight at 4°C. Then, after two rinses for 5 min each with PBS, biotinylated antigoat IgG was added at a dilution of 1:50, followed by incubation for 30 min. The sections were rinsed twice with PBS, and Vectastain Elite ABC Reagent (Vector Laboratories, Burlingame, CA, USA) was added for 30 min. The sections were rinsed again twice with PBS and incubated with the 3,3′-diaminobenzidine tetrahydrochloride (DAB+) Liquid System (Dako, Glostrup, Denmark) for 10 min. Finally, the sections were rinsed and counterstained with hematoxylin solution.

The ORP5 was weakly expressed in the acinar cells of the pancreas and the expression levels of ORP5 in the pancreatic cancer specimens were analyzed by comparison with those in the acinar cells. The expression status of ORP5 was specified as follows: (1) ORP5-negative: the staining intensity in pancreatic cancer tissue was less than that in the acinar cells, and (2) ORP5-positive: the staining intensity in pancreatic cancer tissue was greater than that in the acinar cells.

doi: 10.1111/j.1349-7006.2008.00987.x

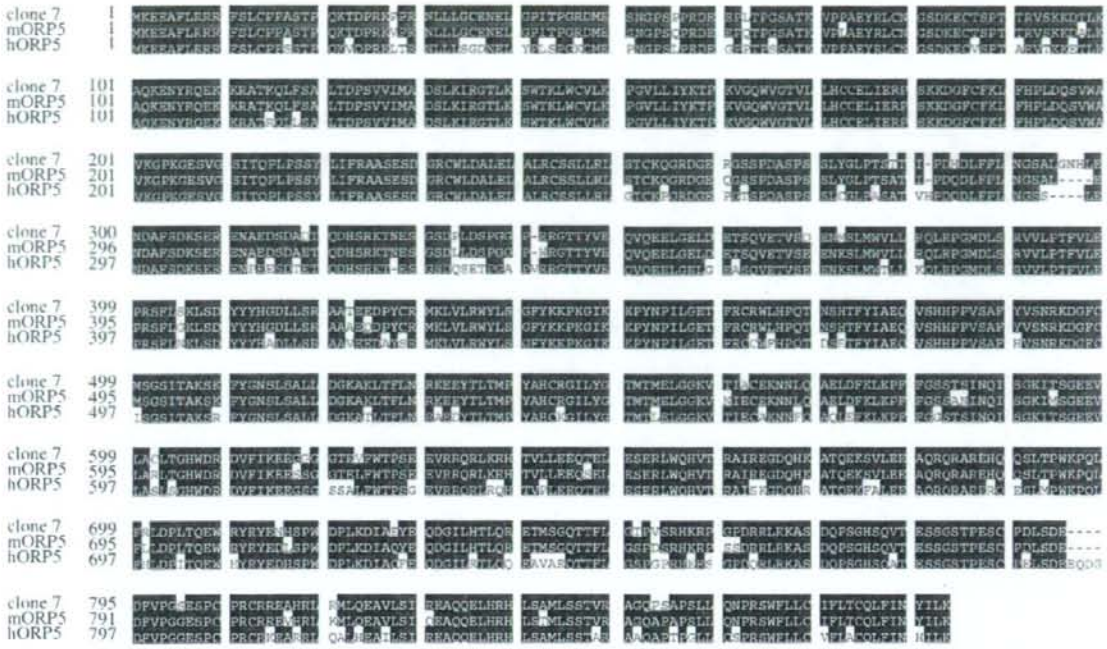

Fig. 1. Homology of clone 7 and mouse human oxysterol binding protein-related protein (ORP)-5. Open reading frame of clone 7 consisting of 878 amino acids. Clone 7 was found to exhibit 95% homology at the amino acid level to mouse ORP5 (mORP5), and 85% homology at the amino acid level to human ORP5 (hORP5).

Statistical analysis. The data analyses were carried out using StatView Ver. 5 for Windows (Abacus Concepts, Inc., Berkeley, CA). The invasion assay was analyzed by two-sided Student's *t*-test. The statistical differences in the expression levels of ORP5 and the pathological characteristics were determined by the chi-square test. Overall survival was calculated from the date of surgical operation to the date of death. Data were plotted to obtain Kaplan-Meier curves, and the median survival time and one-year survival rate were analyzed by the Breslow-Gehan-Wilcoxon test. Values of $P < 0.05$ were considered to be statistically significant.

Results

Isolation of the unknown gene. In our previous report, five clones were either specifically or highly expressed in the PC1.0 cells compared with the PC1 cells,[6] and three of these clones showed no significant homology with known genes. By library screening and 5′ RACE, we successfully isolated one clone (clone 7) with an open reading frame of 2637 nucleotides and 878 amino acids. These sequence data have been submitted to the DNA Data Bank of Japan, European Molecular Biology Laboratory, and GenBank databases under accession number EU475903. According to the database, this gene was found to exhibit 93% homology at the nucleotide level and 95% homology at the amino acid level to mouse *ORP5*, and 86% homology at the nucleotide level and 85% homology at the amino acid level to human *ORP5* (Fig. 1).

ORP5 suppression and induction. Strong expression of ORP5 mRNA was found in the PC1.0, Capan1, Capan2, and Panc1 cells, moderate expression was found in the MiaPaCa2 cells, and weak expression was found in the PC1 and Hs700T cells. A similar expression pattern was observed at the protein level (Fig. 2a,b). For the expression patterns of human ORP5, Capan2 and Hs700T cells were used as human pancreatic cancer cell lines showing high and low expression levels of ORP5, respectively. Transfection of ORP5 siRNA into PC1.0 and Capan2 cells resulted in a significant decrease in the expression level of ORP5 at 48–72 h after the transfection. However, there was no significant difference in the expression level of ORP5 between PC1.0 cells and PC1.0 cells transfected with control siRNA, or between Capan2 cells and Capan2 cells transfected with control siRNA (Fig. 2a,c). Transfection of pcDNA/hamORP5 into PC1 cells or of pcDNA/huORP5 into Hs700T cells resulted in a significant increase in the expression level of ORP5 at 24–72 h after the transfection. However, there was no difference in the ORP5 expression level between PC1 cells and PC1 cells transfected with pcDNA/LacZ, or between Hs700T cells and Hs700T cells transfected with pcDNA/LacZ (Fig. 2a,c). The ORP5 stable transfectant cells (PC1 + ORP5 or Hs700T + ORP5) showed high expression levels of ORP5, whereas the LacZ stable transfectant cells (PC1 + LacZ or Hs700T + LacZ) showed weak expression of ORP5 (Fig. 2d). Cell growth and morphology did not change after ORP5 suppression or induction (data not shown).

Invasion assay of PC1.0, PC1, Capan2, and Hs700T cells after suppression or induction of ORP5. Cell dissociation and migration would be the initial step for invasion. Therefore, we investigated the invasiveness of the pancreatic cancer cells after suppression or induction of ORP5. The invasive cell count in each cell line was compared with that in untreated cells. The invasion cell rates in the untreated PC1.0, PC1.0-ORP5, and PC1.0-control cells were (mean ± SD) 100.0 ± 42.3, 27.1 ± 21.3, and 81.9 ± 25.9%, respectively. ORP-5 suppression resulted in a significant decrease

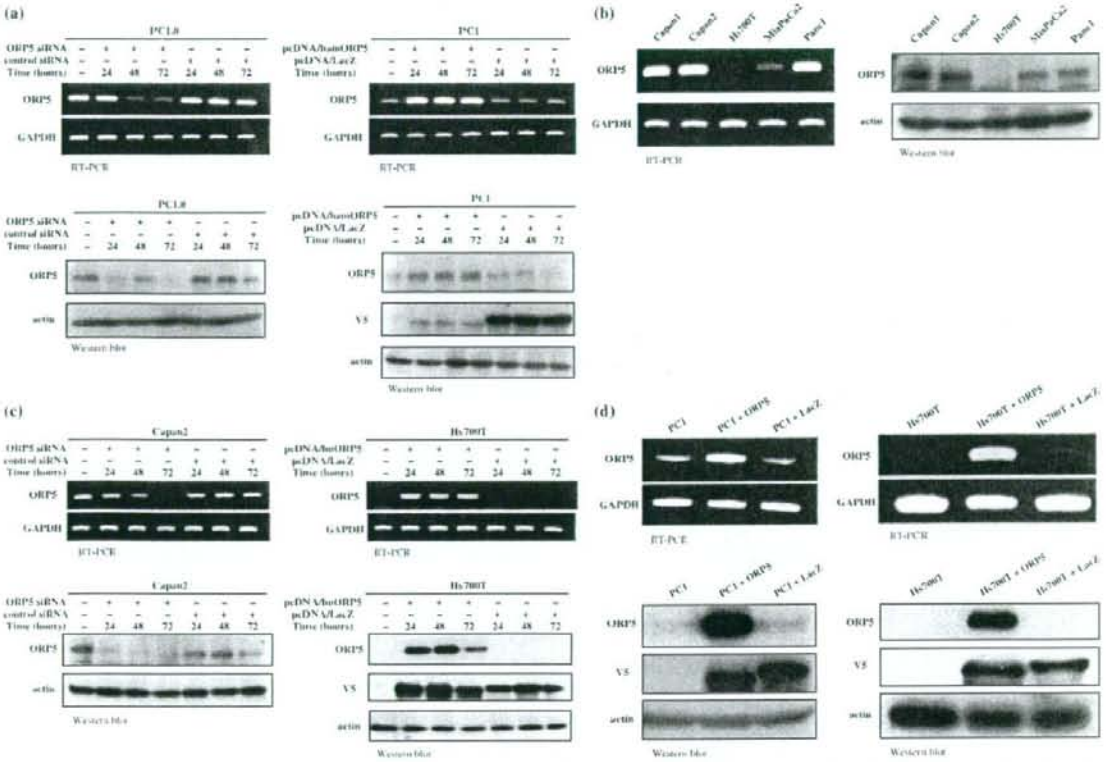

Fig. 2. Expression levels of oxysterol binding protein-related protein (ORP)-5 in hamster and human pancreatic cancer cell lines. PC1 was hamster pancreatic cancer cell line with a low potential for invasion and metastasis, and PC1.0 was hamster pancreatic cancer cell line with a high potential for invasion and metastasis. (a) ORP5 expression in the hamster pancreatic cancer cell lines PC1.0 and PC1 after transfection of short interfering RNA (siRNA) or expression vector. ORP5 was expressed at a high level in the PC1.0 cells and at a low level in the PC1 cells, at both the mRNA and protein levels. Transfection of ORP5 siRNA into PC1.0 cells resulted in a significant decrease in the expression level of ORP5 at 48–72 h after transfection. Transfection of pcDNA/hamORP5 into PC1 cells resulted in a significant increase in the expression level of ORP5 at 24–72 h after transfection. (b) The expression levels of ORP5 in human pancreatic cancer cell lines. At both the mRNA and protein level, ORP5 was expressed at a high level in Capan1, Capan2, and Panc1 cells, at a moderate level in the MiaPaCa2 cells, and at a low level in the Hs700T cells. (c) ORP5 expression in the human pancreatic cancer cell lines Capan2 and Hs700T after transfection of siRNA or expression vector. ORP5 was expressed at a high level in the Capan2 cells, but at a low level in the Hs700T cells, at both the mRNA and protein levels. Transfection of ORP5 siRNA into Capan2 cells resulted in a significant decrease in the expression level of ORP5 at 48–72 h after transfection. Transfection of pcDNA/huORP5 into Hs700T cells resulted in a significant increase in the expression level of ORP5 at 24–72 h after transfection. (d) The ORP5 stable transfectant cells (PC1 + ORP5 or Hs700T + ORP5) showed high expression levels of ORP5, and the LacZ stable transfectant cells (PC1 + LacZ or Hs700T + LacZ) showed low expression levels of ORP5. GAPDH, glyceraldehyde 3-phosphate dehydrogenase; RT-PCR, reverse transcription–polymerase chain reaction.

in cell invasion compared with untreated PC1.0 ($P < 0.0001$) and PC1.0-control cells ($P = 0.0005$) (Fig. 3a). An invasion assay was also carried out for PC1, PC1 + ORP, and PC1 + LacZ. The cell invasion rates in the untreated PC1, PC1 + ORP, and PC1 + LacZ cells were (mean ± SD) 100.0 ± 20.5, 385.1 ± 35.2, and 104.3 ± 19.5%, respectively. ORP5 induction resulted in a significant increase in cell invasion compared with untreated PC1 ($P < 0.0001$) and PC1 + LacZ cells ($P < 0.0001$) (Fig. 3b).

The invasiveness of human pancreatic cancer cells was also analyzed. The invasion cell rates in untreated Capan2, Capan2-ORP5, and Capan2-control cells were (mean ± SD) 100.0 ± 26.9, 63.3 ± 18.2, and 89.5 ± 12.8%, respectively. ORP-5 suppression resulted in a significant decrease in the invasion of cells compared with untreated Capan2 ($P = 0.0015$) and Capan2-control cells ($P = 0.016$) (Fig. 3c). The invasion cell rates in the untreated Ha700T, Hs700T + ORP, and Hs700T + LacZ cells were (mean ± SD) 100.0 ± 28.3, 198.4 ± 75.4, and 74.0 ± 24.9%, respectively. ORP5 induction resulted in a significant increase in the invasion of cells compared with untreated Hs700T ($P < 0.0001$) and Hs700T + LacZ cells ($P < 0.0001$) (Fig. 3d).

Pathological analyses of ORP5 expression levels. Among the 56 pancreatic cancer specimens analyzed, 33 were judged to be ORP5 positive and 23 to be ORP5 negative (Fig. 4; Table 1). With regard to regional invasion, the differences between the ORP5-positive cancers and ORP5-negative cancers were not significant (Table 1). With regard to the surgical margin, 6 of the 32 ORP5-positive pancreatic cancers (18.8%) showed a positive surgical margin whereas none of the 21 ORP5-negative cancers showed a positive surgical margin. A significant difference was seen between the ORP5-positive cancers and ORP5-negative cancers in terms of the positivity of the surgical margin ($P = 0.02$). In the case of a positive surgical margin, the cancer was more invasive to veins (v+; 6/6), nerves (ne+; 6/6), and lymphoducts (ly; 5/6), and few invaded the main pancreas duct (mpd; 1/6).

doi: 10.1111/j.1349-7006.2008.00987.x

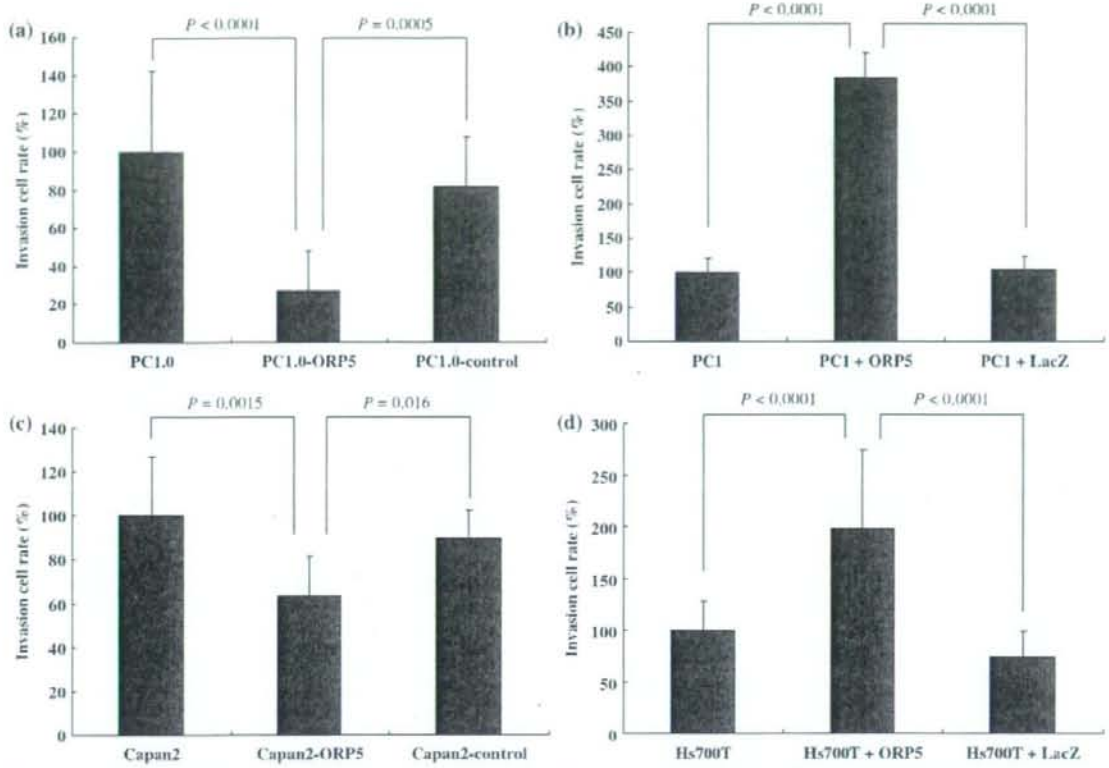

Fig. 3. Invasion assays of hamster and human pancreatic cancer cell lines after suppression or induction of oxysterol binding protein-related protein (ORP)-5. (a) ORP-5 suppression (PC1.0-ORP5) significantly decreased the invasion cell rate compared with untreated PC1.0 ($P < 0.0001$) and PC1.0-control cells ($P = 0.0005$). (b) ORP5 induction (PC1 + ORP5) significantly increased the invasion cell rate compared with untreated PC1 ($P < 0.0001$) and PC1 + LacZ cells ($P < 0.0001$). (c) ORP-5 suppression (Capan2-ORP5) significantly decreased the invasion cell rate compared with untreated Capan2 ($P = 0.0015$) and Capan2-control cells ($P = 0.016$). (d) ORP5 induction (Hs700T + ORP5) significantly increased the invasion cell rate compared with untreated Hs700T ($P < 0.0001$) and Hs700T + LacZ cells ($P < 0.0001$). All results are expressed as invasion cell rate ± SD from three separate experiments.

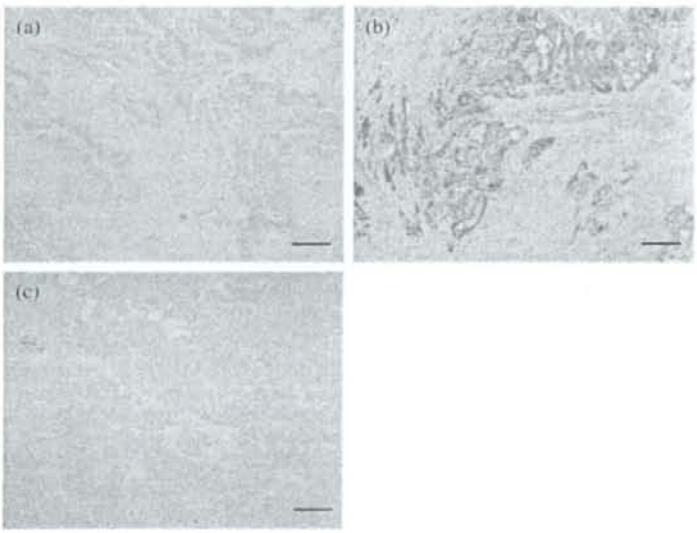

Fig. 4. Immunohistochemical staining of oxysterol binding protein-related protein (ORP)-5. The expression level of ORP5 in pancreatic cancer specimens was analyzed in comparison with that in the acinar cells of the pancreas. (a) ORP5-negative pancreatic cancer tissue. (b) ORP5-positive pancreatic cancer tissue. ORP5 was highly expressed in the cytoplasm of cancer cells. (c) Weak expression of ORP5 in the acinar cells of the pancreas. Scale bar = 100 μm.

Table 1. Pathological characteristics of patients

Characteristics	ORP5 posotive ($n = 33$)	ORP5 negative ($n = 23$)	P-value
Regional invasive factor			
Invasion to the common bile duct in pancreas			0.42
–	18	10	
+	15	13	
Invasion to the duodenum			0.76
–	18	12	
+	14	11	
Invasion to the serosal surface of the pancreas			0.16
–	11	12	
+	22	11	
Invasion to the retroperitoneal surface of the pancreas			0.18
–	9	3	
+	23	20	
Invasion to the intrapancreatic portal vein			0.64
–	18	14	
+	15	9	
Invasion to the artery			0.39
–	30	20	
+	2	3	
Invasion to the main pancreatic duct			0.10
–	20	16	
+	12	3	
Lymphatic invasion			0.37
–	5	6	
+	26	17	
Venous invasion			0.30
–	6	2	
+	26	21	
Neural invasion in pancreas			0.27
–	4	1	
+	26	22	
Surgical margin factor			
Surgical margin of pancreas			0.02
–	21	21	
+	6	0	
Surgical margin of bile duct			0.19
–	25	14	
+	0	1	
Surgical margin of detachment of pancreas			0.59
–	18	15	
+	13	8	
Lymph node metastasis			0.14
–	8	2	
+	25	21	

Pathological analyses were classified according to the Japanese Classification System. The statistical differences between the expression level of oxysterol binding protein-related protein (ORP)-5 and the pathological characteristics were determined by χ^2-test. Values of $P < 0.05$ were considered statistically significant.

One-year survival rate and overall survival of the patients with ORP5-positive and ORP5-negative cancer. Overall survival was calculated from the date of surgical operation to the date of death and data were plotted to obtain Kaplan–Meier curves. The median survival times of all of the patients with ORP5-positive and ORP5-negative cancers were 8.3 and 17.2 months, respectively (Fig. 5a), the difference being significant ($P = 0.02$). The 1-year survival rates of patients with ORP5-positive and ORP5-negative cancers were 36.4 and 73.9%, respectively, the difference again being significant ($P = 0.005$). Meanwhile, the 3-year survival rate of the patients with ORP5-positive cancer and ORP5-negative cancer were 6.1 and 8.7%, respectively, the difference not being significant. Overall survival was analyzed in the case of stage I, II, and III pancreatic cancer (Fig. 5b). The median survival times of the patients with stage I, II, and III pancreatic cancer grouped by ORP5-positive and ORP5-negative were 6.7 and 22.4 months, respectively, the difference being significant ($P = 0.018$). Overall survival was also analyzed in the case of stage IVa and IVb pancreatic cancer (Fig. 5c). The median survival times of the patients with stage IVa and IVb pancreatic cancer grouped as ORP5-positive and ORP5-negative were 9.6 and 14.8 months, respectively, the difference not being significant ($P = 0.27$).

Discussion

Recently, many reports have been published concerning the mechanisms of actions of OSBP and the ORP family. ORP5 is a member of the ORP family, which has been reported to be encoded by 12 genes in humans.[14,15] OSBP is the first protein identified as a receptor for the endogenous oxysterols,[16,17] and it has been cloned and reported to be conserved from *Saccharomyces cerevisiae* to *Homo sapiens*.[30–32] OSBP is a mammalian cytosolic protein that binds to 25-hydroxycholesterol and translocates to the membranes of the Golgi apparatus.[18–20] This membrane interaction is mediated by the pleckstrin homology (PH) domain located in the N-terminal region of the protein.[33–36] OSBP has been reported to be involved in vesicle transport, lipid metabolism, and signal transduction.[21–28]

Although these molecules are now one of the main subjects of study in the field of lipid metabolism, we detected one of these genes (*ORP5*) in a very different context. In a recent study, we compared two hamster pancreatic cancer cell lines with different potentials for invasion and metastasis, detected five mRNA fragments expressed differentially in these cells by RDA,[6] and identified one of these genes as *ORP5*. There are several reports concerning the relationship of ORP with malignancy, including chronic myeloid leukemia,[37] B-cell lymphoma,[38–41] testicular cancer,[42–44] and cholangiocarcinoma.[45] It has been demonstrated that *ORP8* is expressed at a higher level in hamster cholangiocarcinoma compared with normal liver.[45] It is worthy of note that *ORP5* and *ORP8* belong to the same subfamily that carries a putative transmembrane domain sequence at the C-terminal end;[14,15] however, the relationship between *ORP8* and cancer progression or cancer invasion has not yet been assessed. To the best of our knowledge, this is the first report to demonstrate a clear relationship between one of the ORP family genes and cancer invasion, and also that the expression of this molecule is related to survival in cancer patients.

We demonstrated a clear relationship between ORP5 expression and cancer invasion *in vitro* (Fig. 3). Unexpectedly, however, there was no significant difference between ORP5-positive cancer and ORP5-negative cancer among human pancreatic cancer tissue specimens in terms of the regional invasive factor (Table 1). One of the reasons for this could be that almost all of the pancreatic cancer tissue specimens in the present study were positive for regional invasive factor. In cases with a positive surgical margin, all of the patients were ORP5-positive and the cancer tissue specimens tended to be positive for regional invasive factor, except the main pancreas duct (mpd+; 1/6). This result lends support to the idea that ORP5 is related to invasion in human pancreatic cancer.

With regard to survival, the 2-year, 3-year, and 5-year survival rates were 15.2, 6.1, and 3.0% in ORP5-positive cancer, and 21.7, 8.7, and 8.7% in ORP5-negative cancer (Fig. 5a). Although

doi: 10.1111/j.1349-7006.2008.00987.x

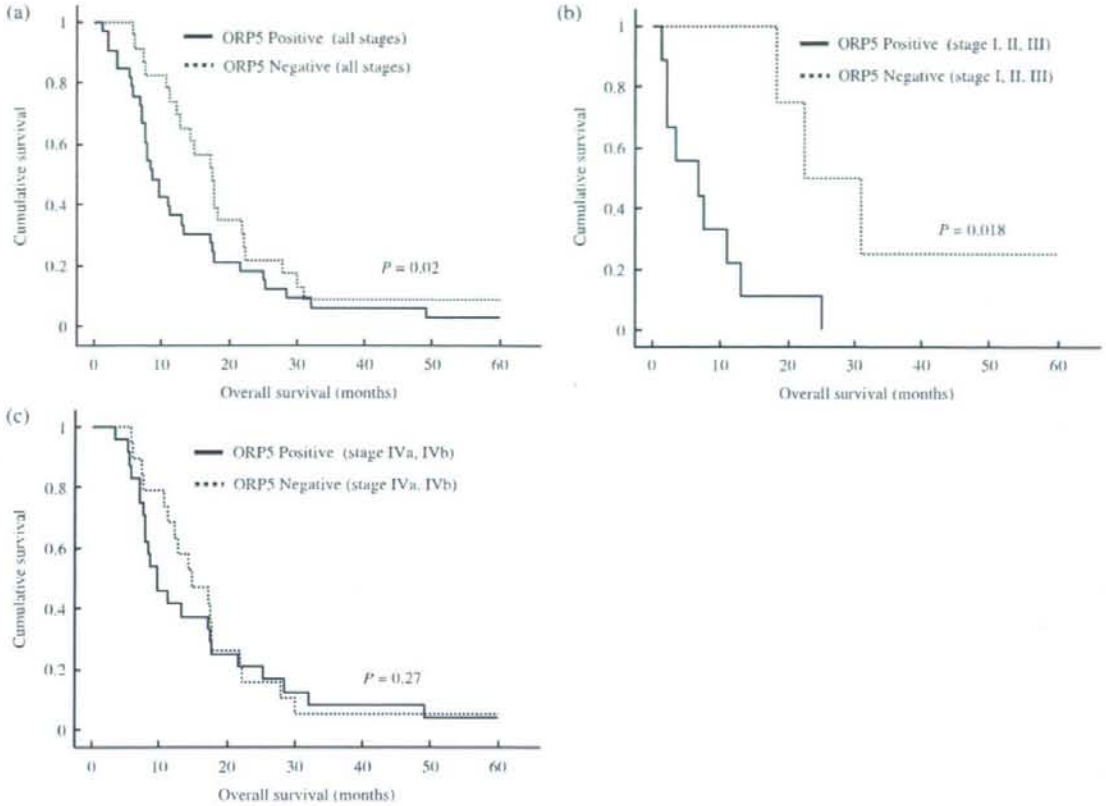

Fig. 5. Overall survival stratified by oxysterol binding protein-related protein (ORP)-5 expression status. (a) Kaplan–Meier plot of overall survival of all patients with pancreatic cancer grouped by ORP5 expression status (ORP5-positive and ORP5-negative). The median survival times of the patients with ORP5-positive cancer ($n = 33$) and ORP5-negative cancer ($n = 23$) were 8.3 and 17.2 months, respectively, and the 1-year survival rates were 36.4 and 73.9%, respectively. (b) Kaplan–Meier plot of overall survival of patients with stage I, II, and III of pancreatic cancer grouped by ORP5 expression status. The median survival times of the patients with ORP5-positive cancer ($n = 9$) and ORP5-negative cancer ($n = 4$) were 6.7 and 22.4 months, respectively. (c) Kaplan–Meier plot of overall survival of patients with stage IVa and IVb pancreatic cancer grouped by ORP5 expression status. The median survival times of patients with ORP5-positive cancer ($n = 24$) and ORP5-negative cancer ($n = 19$) were 9.6 and 14.8 months, respectively.

the long-term survival rate tended to be better in the ORP5-negative group, the difference was not significant. However, the 1-year survival rate and median survival time were 73.9% and 17.2 months, respectively, in the ORP5-positive group, and 36.4% and 8.3 months, respectively, in the ORP5-negative group. Significant differences were observed in the 1-year survival rate ($P = 0.005$) and median survival time ($P = 0.02$) between the two groups. In particular, as pancreatic cancer is a type of cancer with poor prognosis compared to other cancers, it is noteworthy that the median survival time of the ORP5-negative group was longer than that of the ORP5-positive group by 8.9 months. Furthermore, in the case of stage I, II, and III pancreatic cancer, the ORP5-negative group had a better prognosis than the ORP5-positive group (Fig. 5b). From these results, although the mechanisms of ORP5 expression in cancer invasion are still not very clear, we concluded that this molecule is related to cancer invasion, and is associated with a high invasion rate to the main pancreas duct, which eventually leads to early relapse and short survival.

In the present study, it was of interest that ORP5, which was isolated from a hamster pancreatic cancer cell line with a high potential for invasion and metastasis, is related to the invasion and poor prognosis of human pancreatic cancer. Before evaluating pancreatic cancer samples, we assessed normal human samples by immunohistochemistry. The expression patterns of ORP5 were as follows: (1) no expression in heart and muscle; (2) slight expression in purkinje cells of the brain, parts of the spleen and kidney, acinar cells of the pancreas, and epithelial cells of the lung; and (3) strong expression in the liver (data not shown). Unfortunately, we assume that targeting this molecule directly for cancer therapy is not possible.

Further investigations are necessary to elucidate the mechanism regulating pancreatic cancer invasion and metastasis. Isolation of the other two unknown genes may provide valuable insight into the signal transduction processes involved in invasion and metastasis. Furthermore, these results could pave the way for the development of new therapeutic methods based on inhibition of target genes related to tumor cell invasion and metastasis.

Acknowledgments

The present study was supported by a Grant-in-Aid from the Ministry of Education, Culture, and Science of Japan.

References

1 Pour PM, Egami H, Takiyama Y. Patterns of growth and metastases of induced pancreatic cancer in relation to the prognosis and its clinical implications. *Gastroenterology* 1991; **100**: 529–36.
2 Egami H, Takiyama Y, Cano M, Houser WH, Pour PM. Establishment of hamster pancreatic ductal carcinoma cell line (PC-1) producing blood group-related antigens. *Carcinogenesis* 1989; **10**: 861–9.
3 Egami H, Tomioka T, Tempero M, Kay D, Pour PM. Development of intrapancreatic transplantable model of pancreatic duct adenocarcinoma in Syrian golden hamsters. *Am J Pathol* 1991; **138**: 557–61.
4 Hirota M, Egami H, Corra S *et al*. Production of scatter factor-like activity by a nitrosamine-induced pancreatic cancer cell line. *Carcinogenesis* 1993; **14**: 259–64.
5 Kurizaki T, Egami H, Hirota M *et al*. Characterization of cancer cell dissociation factor in a highly invasive pancreatic cancer cell line. *Cancer* 1995; **75**: 1554–61.
6 Ishikawa S, Egami H, Kurizaki T *et al*. Identification of genes related to invasion and metastasis in pancreatic cancer by cDNA representational difference analysis. *J Exp Clin Cancer Res* 2003; **22**: 299–306.
7 Tan X, Egami H, Kamohara H *et al*. Involvement of the mitogen-activated protein kinase kinase 2 in the induction of cell dissociation in pancreatic cancer. *Int J Oncol* 2004; **24**: 65–73.
8 Tan X, Egami H, Ishikawa S *et al*. Relationship between the expression of extracellular signal-regulated kinase 1/2 and the dissociation of pancreatic cancer cells: involvement of ERK1/2 in the dissociation status of cancer cells. *Int J Oncol* 2004; **24**: 815–20.
9 Tan X, Tamori Y, Egami H *et al*. Analysis of the invasion–metastasis mechanism in pancreatic cancer: involvement of tight junction transmembrane protein occludin and MEK/ERK signal transduction pathway in cancer cell dissociation. *Oncol Rep* 2004; **11**: 993–8.
10 Tan X, Egami H, Ishikawa S *et al*. Relationship between activation of epidermal growth factor receptor and cell dissociation in pancreatic cancer. *Int J Oncol* 2004; **25**: 1303–9.
11 Tan X, Egami H, Ishikawa S *et al*. Arrangement of expression and distribution of tight junction protein claudin-1 in cell dissociation of pancreatic cancer cells. *Int J Oncol* 2004; **25**: 1567–74.
12 Tan X, Egami H, Ishikawa S *et al*. Involvement of matrix metalloproteinase-7 in invasion–metastasis through induction of cell dissociation in pancreatic cancer. *Int J Oncol* 2005; **26**: 1283–9.
13 Tan X, Egami H, Ishikawa S, Kurizaki T, Hirota M, Ogawa M. Zonula occludens-1 (ZO-1) redistribution is involved in the regulation of cell dissociation in pancreatic cancer cells. *Dig Dis Sci* 2005; **50**: 1402–9.
14 Lehto M, Laitinen S, Chinetti G *et al*. The OSBP-related protein family in humans. *J Lipid Res* 2001; **42**: 1203–13.
15 Jaworski CJ, Moreira E, Li A, Lee R, Rodriguez IR. A family of 12 human genes containing oxysterol-binding domains. *Genomics* 2001; **78**: 185–96.
16 Taylor FR, Saucier SE, Shown EP, Parish EJ, Kandutsch AA. Correlation between oxysterol binding to a cytosolic binding protein and potency in the repression of hydroxymethylglutaryl coenzyme A reductase. *J Biol Chem* 1984; **259**: 12 382–7.
17 Taylor FR, Kandutsch AA. Oxysterol binding protein. *Chem Phys Lipids* 1985; **38**: 187–94.
18 Ridgway ND, Dawson PA, Ho YK, Brown MS, Goldstein JL. Translocation of oxysterol binding protein to Golgi apparatus triggered by ligand binding. *J Cell Biol* 1992; **116**: 307–19.
19 Perry RJ, Ridgway ND. Oxysterol-binding protein and vesicle-associated membrane protein-associated protein are required for sterol-dependent activation of the ceramide transport protein. *Mol Biol Cell* 2006; **17**: 2604–16.
20 Suchanek M, Hynynen R, Wohlfahrt G *et al*. The mammalian oxysterol-binding protein-related proteins (ORPs) bind 25-hydroxycholesterol in an evolutionarily conserved pocket. *Biochem J* 2007; **405**: 473–80.
21 Hynynen R, Laitinen S, Kakela R *et al*. Overexpression of OSBP-related protein 2 (ORP2) induces changes in cellular cholesterol metabolism and enhances endocytosis. *Biochem J* 2005; **390**: 273–83.
22 Lehto M, Olkkonen VM. The OSBP-related proteins: a novel protein family involved in vesicle transport, cellular lipid metabolism, and cell signalling. *Biochim Biophys Acta* 2003; **1631**: 1–11.
23 Wang PY, Weng J, Anderson RG. OSBP is a cholesterol-regulated scaffolding protein in control of ERK 1/2 activation. *Science* 2005; **307**: 1472–6.
24 Im YJ, Raychaudhuri S, Prinz WA, Hurley JH. Structural mechanism for sterol sensing and transport by OSBP-related proteins. *Nature* 2005; **437**: 154–8.
25 Massey JB. Membrane and protein interactions of oxysterols. *Curr Opin Lipidol* 2006; **17**: 296–301.
26 Fairn GD, Curwin AJ, Stefan CJ, McMaster CR. The oxysterol binding protein Kes1p regulates Golgi apparatus phosphatidylinositol-4-phosphate function. *Proc Natl Acad Sci USA* 2007; **104**: 15 352–7.
27 Lessmann E, Ngo M, Leitges M, Minguet S, Ridgway ND, Huber M. Oxysterol-binding protein-related protein (ORP) 9 is a PDK-2 substrate and regulates Akt phosphorylation. *Cell Signal* 2007; **19**: 384–92.
28 Yan D, Lehto M, Rasilainen L *et al*. Oxysterol binding protein induces upregulation of SREBP-1c and enhances hepatic lipogenesis. *Arterioscler Thromb Vasc Biol* 2007; **27**: 1108–14.
29 Japan Pancreas Society. *Classification of Pancreatic Carcinoma*, 2nd English edn. Tokyo: Kanehara & Co., 2003.
30 Dawson PA, Ridgway ND, Slaughter CA, Brown MS, Goldstein JL. cDNA cloning and expression of oxysterol-binding protein, an oligomer with a potential leucine zipper. *J Biol Chem* 1989; **264**: 16 798–803.
31 Levanon D, Hsieh CL, Francke U *et al*. cDNA cloning of human oxysterol-binding protein and localization of the gene to human chromosome 11 and mouse chromosome 19. *Genomics* 1990; **7**: 65–74.
32 Olkkonen VM, Levine TP. Oxysterol binding proteins: in more than one place at one time? *Biochem Cell Biol* 2004; **82**: 87–98.
33 Lagace TA, Byers DM, Cook HW, Ridgway ND. Altered regulation of cholesterol and cholesteryl ester synthesis in Chinese hamster ovary cells overexpressing the oxysterol-binding protein is dependent on the pleckstrin homology domain. *Biochem J* 1997; **326**: 205–13.
34 Levine TP, Munro S. The pleckstrin homology domain of oxysterol-binding protein recognises a determinant specific to Golgi membranes. *Curr Biol* 1998; **8**: 729–39.
35 Balla A, Tuymetova G, Tsiomenko A, Varnai P, Balla T. A plasma membrane pool of phosphatidylinositol 4-phosphate is generated by phosphatidylinositol 4-kinase type-III alpha: studies with the PH domains of the oxysterol binding protein and FAPP1. *Mol Biol Cell* 2005; **16**: 1282–95.
36 Wang PY, Weng J, Lee S, Anderson RG. The N terminus controls sterol binding while the C terminus regulates the scaffolding function of OSBP. *J Biol Chem* 2008; **283**: 8034–45.
37 Pizzatti L, Sa LA, de Souza JM, Bisch PM, Abdelhay E. Altered protein profile in chronic myeloid leukemia chronic phase identified by a comparative proteomic study. *Biochim Biophys Acta* 2006; **1764**: 929–42.
38 Ando T, Suguro M, Kobayashi T, Seto M, Honda H. Multiple fuzzy neural network system for outcome prediction and classification of 220 lymphoma patients on the basis of molecular profiling. *Cancer Sci* 2003; **94**: 906–13.
39 Sander B, Flygare J, Porwit-Macdonald A *et al*. Mantle cell lymphomas with low levels of cyclin D1 long mRNA transcripts are highly proliferative and can be discriminated by elevated cyclin A2 and cyclin B1. *Int J Cancer* 2005; **117**: 418–30.
40 Chng WJ, Schop RF, Price-Troska T *et al*. Gene-expression profiling of Waldenstrom macroglobulinemia reveals a phenotype more similar to chronic lymphocytic leukemia than multiple myeloma. *Blood* 2006; **108**: 2755–63.
41 Ek S, Andreasson U, Hober S *et al*. From gene expression analysis to tissue microarrays: a rational approach to identify therapeutic and diagnostic targets in lymphoid malignancies. *Mol Cell Proteomics* 2006; **5**: 1072–81.
42 Sperger JM, Chen X, Draper JS *et al*. Gene expression patterns in human embryonic stem cells and human pluripotent germ cell tumors. *Proc Natl Acad Sci USA* 2003; **100**: 13 350–5.
43 Gashaw I, Grummer R, Klein-Hitpass L *et al*. Gene signatures of testicular seminoma with emphasis on expression of ets variant gene 4. *Cell Mol Life Sci* 2005; **62**: 2359–68.
44 Juric D, Sale S, Hromas RA *et al*. Gene expression profiling differentiates germ cell tumors from other cancers and defines subtype-specific signatures. *Proc Natl Acad Sci USA* 2005; **102**: 17 763–8.
45 Loilome W, Yongvanit P, Wongkham C *et al*. Altered gene expression in *Opisthorchis viverrini*-associated cholangiocarcinoma in hamster model. *Mol Carcinog* 2006; **45**: 279–87.

doi: 10.1111/j.1349-7006.2008.00987.x

Expression patterns of epiplakin1 in pancreas, pancreatic cancer and regenerating pancreas

Tetsu Yoshida[1], Nobuaki Shiraki[1], Hideo Baba[2], Mizuki Goto[3], Sakuhei Fujiwara[3], Kazuhiko Kume[1] and Shoen Kume[1,4]*

[1]*Division of Stem Cell Biology, Department of Regeneration Medicine, Institute of Molecular Embryology and Genetics (IMEG), and*
[2]*Department of Gastroenterological Surgery, and*
[4]*Global COE, Kumamoto University, Honjo 2-2-1, Kumamoto 860-0811, Japan*
[3]*Department of Anatomy, Biology and Medicine (Dermatology), Faculty of Medicine, Oita University, Hasama-machi, Yufu 879-5593, Japan*

Epiplakin1 (Eppk1) is a plakin family gene with its function remains largely unknown, although the plakin genes are known to function in interconnecting cytoskeletal filaments and anchoring them at plasma membrane-associated adhesive junction. Here we analyzed the expression patterns of Eppk1 in the developing and adult pancreas in the mice. In the embryonic pancreas, Eppk1+/Pdx1+ and Eppk1+/Sox9+ pancreatic progenitor cells were observed in early pancreatic epithelium. Since Pdx1 expression overlapped with that of Sox9 at this stage, these multipotent progenitor cells are Eppk1+/Pdx1+/Sox9+ cells. Then Eppk1 expression becomes confined to Ngn3+ or Sox9+ endocrine progenitor cells, and p48+ exocrine progenitor cells, and then restricted to the duct cells and α cells at birth. In the adult pancreas, Eppk1 is expressed in centroacinar cells (CACs) and in duct cells. Eppk1 is observed in pancreatic intraepithelial neoplasia (PanIN), previously identified as pancreatic ductal adenocarcinoma (PDAC) precursor lesions. In addition, the expansion of Eppk1-positive cells occurs in a caerulein-induced acute pancreatitis, an acinar cell regeneration model. Furthermore, in the partial pancreatectomy (Px) regeneration model using mice, Eppk1 is expressed in "ducts in foci", a tubular structure transiently induced. These results suggest that Eppk1 serves as a useful marker for detecting pancreatic progenitor cells in developing and regenerating pancreas.

Introduction

Plakins are large multidomain molecules, which link cytoskeletal elements together and to connect them to junctional complexes, such as desmosomes and hemidesmosomes (Sonnenberg & Liem 2007). Some of the genes belonging to this family, for example, Desmoplakin, Plectin and BPAG1, are well-characterized. Knockout mice of these genes showed phenotypes of skin blistering and embryonic or neonatal lethalities (Guo *et al.* 1995; Smith *et al.* 1996; Gallicano *et al.* 1998). In human, autoimmune diseases of these genes are reported, consistent with the skin blistering phenotype of the gene knockout mice. Epiplakin1 (Eppk1) is one of the plakin family genes and is involved in the formation of intermediate filament network by binding with keratin and vimentin (Jang *et al.* 2005). Eppk1 was originally cloned as an autoantigen of a human subepidermal blistering disease (Fujiwara *et al.* 2001; Spazierer *et al.* 2003). However, Eppk1 deficient mice develop normally without an evident epidermal phenotype (Goto *et al.* 2006; Spazierer *et al.* 2006), leaving its function *in vivo* elusive. Eppk1 was identified as one of the proteins binding to EGF receptor by proteomics (Blagoev *et al.* 2003), thus suggesting its novel function as a component of EGF signaling.

Eppk1 was reported to be expressed in the pancreas by Northern blot analysis or immunohistochemistry (Fujiwara *et al.* 2001; Spazierer *et al.* 2003), and EGF signaling was reported to be involved in the development of pancreas (Miettinen *et al.* 2000) and carcinogenesis (Miyamoto *et al.* 2003). In an attempt to gain insights into the potential function of Eppk1, the expression of Eppk1 with respect to markers for pancreatic progenitors and differentiated cell types during embryonic development and in regenerating pancreas were carried out. Eppk1

Communicated by: Shinichi Aizawa
**Correspondence*: Email: skume@kumamoto-u.ac.jp

DOI: 10.1111/j.1365-2443.2008.01196.x

was expressed in pancreatic progenitor cells in the early embryos as well as in centroacinar cells (CACs) in adult pancreas. The results suggested that Eppk1 is useful as a marker for progenitor cells in developing and regenerating pancreas.

Results

Expression pattern analyses of Eppk1 in embryo and adult pancreas

Eppk1 expression was first examined with respect to Pdx1, a pancreatic progenitor marker. In this study, two kinds of anti-Eppk1 antibodies raised against distinct epitopes within Eppk1 (Fujiwara *et al.* 2001; Spazierer *et al.* 2003) were used to detect the expression of Eppk1. Both anti-Eppk1 antibodies gave almost the same results and did not recognize any proteins in *Eppk1* KO mice (data not shown). Since both anti-Eppk1 antibodies and anti-Pdx1 antibody were raised in rabbits, a *Pdx1*/green fluorescent protein (GFP) transgenic mouse line in which GFP was driven under the *Pdx1* promoter was used to examine the co-expression of Eppk1 and Pdx1. The expression of GFP completely overlapped with that of Pdx1 in the *Pdx1*/GFP transgenic mice throughout their lifetimes (Fig. S1 in Supplementary Material). Eppk1 expression was found in *Pdx1*/GFP-positive (*Pdx1*/GFP+) pancreatic progenitor cells in the E10.5 pancreas epithelium (Fig. 1A–C). The expression of Eppk1 is also examined with respect to Sox9, a Sry/HMG box transcription factor shown to mark a population of Pdx1+ cells and be required for the maintenance of the progenitor cell pool (Seymour *et al.* 2007). Eppk1 was found to co-localize with Sox9 at this stage (Fig. 1D–F). Therefore, the multipotent progenitor cells are positive for Eppk1, Pdx1 and Sox9 at this stage.

In the E12.5 pancreas epithelium, most cells co-expressed Pdx1 and Eppk1. However, there are a population of Eppk1+ cells, which turned out to be Pdx1-negative (Pdx1−) (arrowheads in Fig. 1G–I) or Sox9− cells (solid lines in Fig. 1J–L). A co-localization of the Sox9 and Pdx1 persisted until this stage (arrows in Supplementary Fig. S2), and Pdx1+/Sox9− cells (arrowheads in Supplementary Fig. S2) begin to emerge. Taken together, the Eppk1+/Pdx1+/Sox9+ cells at E10.5 diverged into Eppk1+/Pdx1−/Sox9− and Eppk1+/Pdx1+/Sox9− cells within the Eppk1+/Pdx1+/Sox9+ pancreatic epithelium at E12.5 (Fig. 8).

In E15.5 pancreas, a divergence of expressions of Eppk1 and *Pdx1*/GFP was observed (Fig. 2A–C). Most of the *Pdx1*/GFP+ cells were Insulin expressing cells at this stage (Supplementary Fig. S3), suggesting these cells are

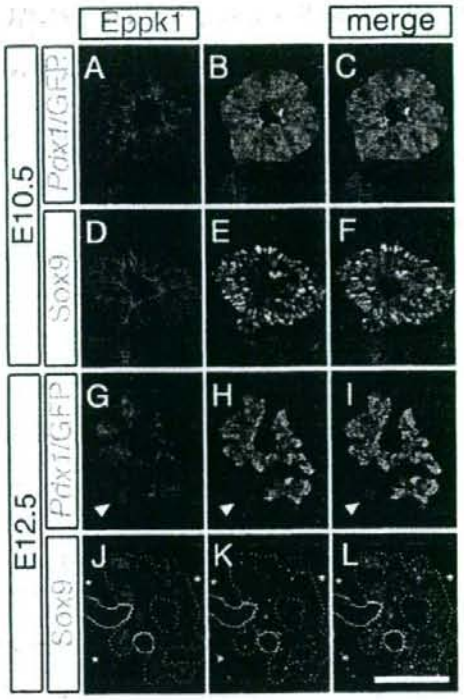

Figure 1 The expression patterns of Eppk1 at early stages of pancreatic development. Immunohistochemical analyses of Eppk1 in E10.5 (A–F) and E12.5 pancreatic buds (G–L). (A, D, G, J) The expressions of Eppk1 (red), (B, H) the images of GFP in *Pdx1*/GFP mice pancreata, (E, K) the expression patterns of Sox9 are shown. The arrowheads in G–I represent Eppk1+*Pdx1*/GFP− cells. The areas surrounded by solid and dotted lines in J–L are Eppk1+/Sox9− cells and Eppk1+/Sox9+ cells, respectively. Asterisks in J–L indicate nonspecific signals. C, F, I and L are merged images. Scale bar, 100 μM (A–F), 170 μM (G–L).

differentiating into β cell lineage. Taken together, the expression of *Pdx1*/GFP is excluded from Eppk1+/Pdx1+/Sox9+ pancreatic progenitor cells. At this stage, Eppk1+/Sox9+ cells retained confined to the "central duct-like structures" (solid lines in Fig. 2) (Seymour *et al.* 2007). Ngn3 was also co-expressed with a population of Eppk1-expressing cells, which reside along the "central duct-like structure" (Fig. 3G–I), indicating the possible endocrine progenitor characteristics of the Sox9+/Eppk1+ cells. On the other hand, in the forming acini (dotted lines in Fig. 2D–F), Sox9 expression decreased, and the expression of p48, which was reported to be expressed in exocrine progenitor cells and to be essential for exocrine

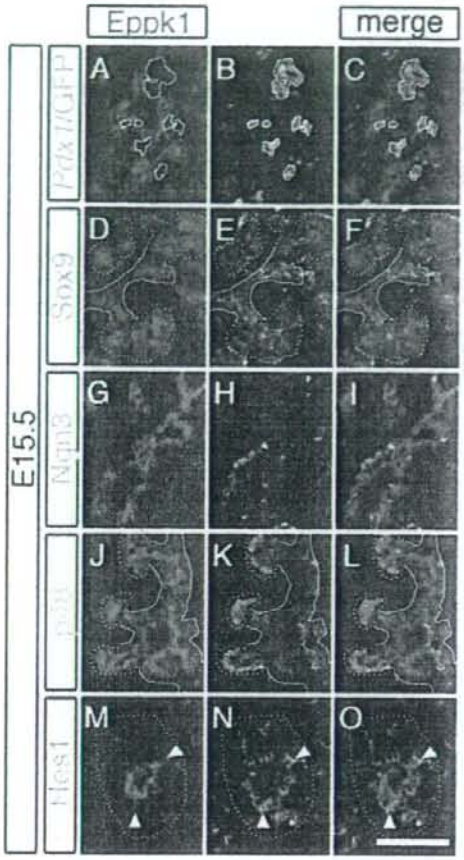

Figure 2 The expression patterns of Eppk1 at secondary transition of pancreatic development. Immunohistochemical analyses of Eppk1 in E15.5 pancreas (A, D, G, J and M). The expression patterns of GFP in *Pdx1*/GFP mouse (B), Sox9 (E), Ngn3 (H), p48 (K) and Hes1 (N) are shown. The areas surrounded by white solid lines in A–C are *Pdx1*/GFP+Eppk1− cells. The areas surrounded by solid and dotted lines in D–O are "central duct-like structure" and forming acini, respectively. The arrowheads in M–O represent centroacinar region. C, F, I, L, and O are merged images. Scale bar, 100 μM (A–L), 30 μM (M–O).

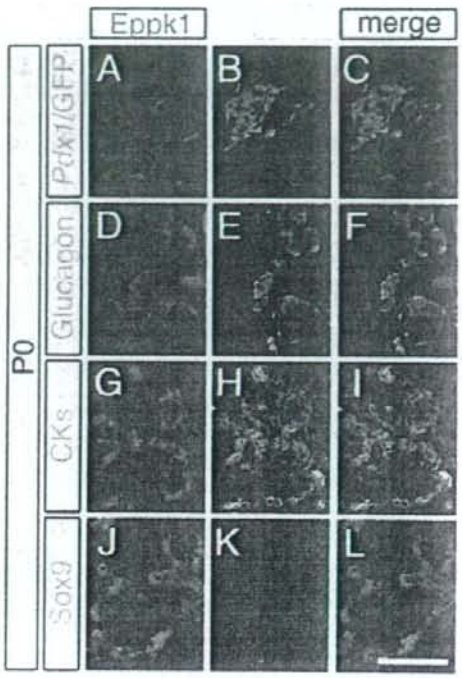

Figure 3 In P0 perinatal pancreas, Eppk1 is expressed in α cells in islets. Immunohistochemical analyses of Eppk1 in P0 pancreas (A, D, G and J). The expression patterns of GFP in *Pdx1*/GFP mouse (B), Glucagon (E), Cytokeratins (H, CKs), Sox9 (K) are shown. C, F, I and L are merged images. Scale bar, 100 μM.

differentiation (Krapp *et al.* 1996, 1998), began to emerge at this stage, which expression found to be co-localized with that of Eppk1 (Fig. 2J–L). Furthermore, Eppk1 expression was observed to co-express with Hes1 in the centroacinar position of the forming acini (Fig. 2M–O) (Esni *et al.* 2004; Jensen 2004). These results thus indicate that Eppk1 is expressed in both endocrine and exocrine progenitor cells at E15.5.

In neonatal pancreas at P0, the expression of Eppk1 no longer overlapped with that of *Pdx1*/GFP (Fig. 3A–C). Eppk1 expression was mainly observed in ducts, with some positive cells in the islets (Fig. 3A–C), which turned out to be Glucagon-expressing α cells (Fig. 3D–F). The expressions of Eppk1 in islets overlapped with that of Cytokeratins (Fig. 3G–I). Cytokeratins were expressed in Glucagon+ cells (Supplementary Fig. S4), which agreed with that reported previously (Bouwens *et al.* 1994). On the other hand, co-expression of Sox9 and Eppk1 was not retained (Fig. 3J–L).

In adult pancreas, Eppk1expressions are observed in relatively small cells surrounded by Amylase+ acinar cells (Fig. 4E,H), but no longer in Glucagon+ α cells (Fig. 4A–C). The Eppk1 expression almost completely overlapped with Cytokeratins (Fig. 3E–H), indicating that they were duct cells. Detailed examination revealed

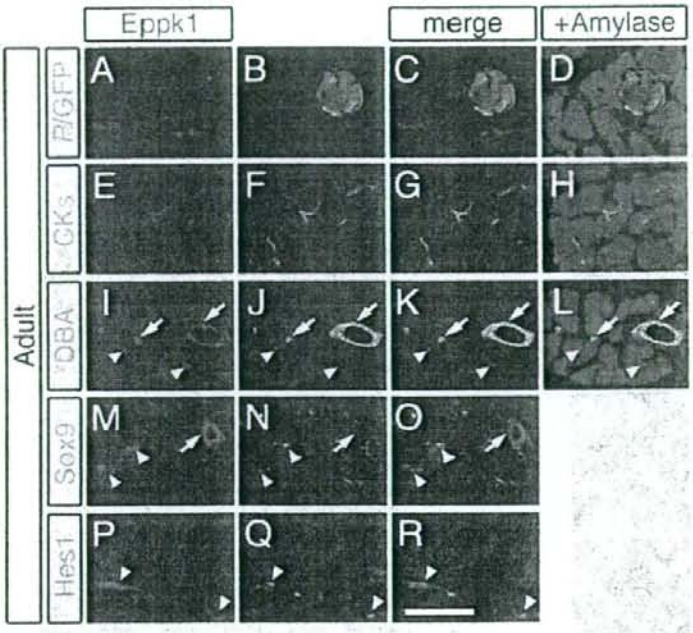

Figure 4 Eppk1 is expressed in duct cells and centroacinar cells of adult pancreas. Immunohistochemical analyses of Eppk1 in adult pancreas (A, E, I, M and P) are shown. The expression patterns of GFP in *Pdx1/* GFP mouse (B), Cytokeratins (F, CKs), Sox9 (N), Hes1 (Q) and DBA+ cells (J) are shown. Arrowheads and arrows in I–L represent the cells lie inside or outside of acinar cells, respectively. Arrowheads and arrows in M–O represent Sox9+ or Sox9– cells, respectively. The arrowheads in P–R are Hes1+/Eppk1+ cells. C, G, K, O and R are merged images. Expressions of Amylase are also shown (D, H and L). Scale bar, 100 μm (A–L), 50 mm (M–R).

that there were two kinds of Eppk1+ cells, one was surrounded by acinar cells (arrowheads in Fig. 4I–L) and the other was outside them (arrows in Fig. 4I–L). The Eppk1+ cells located in the acinar stem position correspond to a terminal ductal position that intercalates with the distal duct cells, and they are called CACs (Slack 1995). The Eppk1+ cells outside acinar cells were duct cells, which could be distinguished by the relatively strong reactivity against DBA, a kind of lectin that binds strongly to duct cells of pancreas, but relatively weakly to CACs (Fig. 4J). In CACs, Eppk1 expression overlapped with Sox9 and Hes1, an effector of Notch signaling (arrowheads in Fig. 4M–R) (Miyamoto *et al.* 2003). In duct cells, only Eppk1, but not Sox9 or Hes1, was detected (arrow in Fig. 4M–O).

Expression patterns of Eppk1 in pancreatic cancer

The next experiment was designed to determine whether Eppk1 was expressed in human pancreatic intraepithelial neoplasia (PanIN) cells, one of the pancreatic ductal adenocarcinoma (PDAC) precursor lesions, because CACs are regarded to be the origin of PanIN (Hezel *et al.* 2006). PanINs are graded from stage 1 to stage 3, increasing grades reflect increasing atypia, and eventually transform into frank PDAC. Normal duct is composed of a single-layer with low cuboidal cells. PanIN1 is considered early cancer precursor lesion, characterized by its columnar and mucinous epithelium (Fig. 5A), which is detected by DBA (Fig. 5C,F), with the nuclei regularly localized along the basement membrane (Fig. 5E,F). In this stage, Eppk1 was expressed in the PanIN cells, which were characterized by the expression of Cytokeratins (Fig. 5G–J). Late PanIN lesions, PanIN2 and PanIN3, represent a distinct step toward invasive carcinoma. The mucinous epithelium becomes thinner, and the epithelium appeared curved with evident invasion beyond the basement membrane as luminal budding (Fig. 5K,P). In late PanINs, the DBA+ epithelium layers become thinner, whereas the DAPI+ cell layers become multilayers (Fig. 3L–P). However, the expressions of Eppk1 and Cytokeratins were down regulated in this stage (Fig. 5Q–T), indicating that PanIN cells lost their ductal characters.

Expression patterns of Eppk1 in regenerating pancreas

CACs are known to be involved not only in the origin of PanIN, but also in the regeneration of acinar cells in acute pancreatitis (Gasslander *et al.* 1992). The next

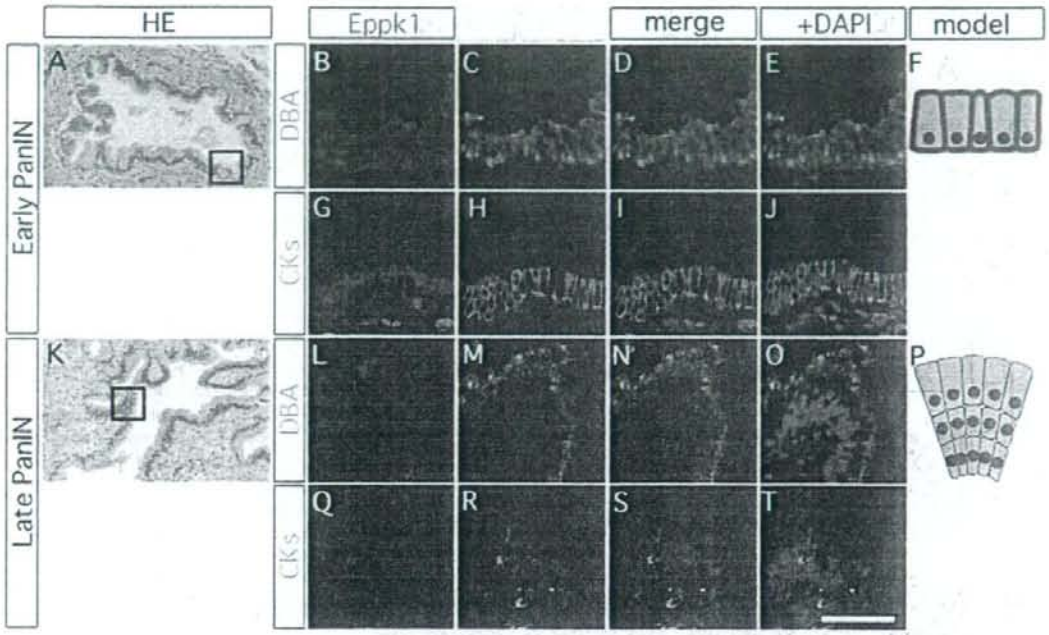

Figure 5 Eppk1 is expressed in the early stage but not in the late stages of PanINs. Histological analyses of the early (A–J) and late stages (K–T) of PanINs. (A, K) Bright-field images of HE-stained PanINs. Boxes in A, K depict regions shown in B–E, or L–T, respectively. The expressions of Eppk1 are examined (B, G, L and Q). DBA+ (C, M) and Cytokeratins+ (H, R; CKs) cells are also shown. D, I, N and S are merged images and blue dots show nuclei (E, J, O and T). Schematic drawings of the intracellular expressions of DBA (green) and Eppk1 (red) are shown in F and P. Scale bar, 400 μM (A, K), 125 μM (B–E, G–J, L–O, Q–T).

question was whether Eppk1+ cells proliferate in regenerating pancreas in acute pancreatitis. Caerulein-mediated pancreatitis has been shown to trigger acinar cell regeneration. We induced weak pancreatitis by caerulein injection (Jensen *et al.* 2005). One day after caerulein injection, acinar cell degeneration began to occur, and the acinar cells thereafter regenerated and almost completely recovered in one week after the initial injection (Fig. 6A–L), and the number of Eppk1+ cells increased by a factor of 1.97 (Supplementary Fig. S5 show low-magnification pictures; compare Supplementary Fig. S5C,D with Supplementary Fig. S5A,B). This resulted in a change in the cellular alignment from linear before treatment into a cluster of cells (compare Fig. 6F with Fig. 6B). At day 7 after the caerulein injection, they almost returned to their original linear alignments, though many cells remained clustered (compare Fig. 6J with Fig. 6B). We next examined the Eppk1+ cells during this regenerating period (Fig. 6M–X). Cytokeratins were still expressed in Eppk1+ cells at day 4 after the caerulein injection (Fig. 6O,P), though most of the Eppk1+ cells lost the reactivity with DBA (Fig. 6Q,R). The co-expressions of Eppk1 with PCNA (Fig. 6S,T) and Sox9 (Fig. 6U,V) indicated that the Eppk1+ cells proliferated and had multipotency (Seymour *et al.* 2007). p48, a marker for acinar progenitor cells, was expressed in Eppk1+ cells with acinar morphology (arrowheads in Fig. 6W,X), thus suggesting a dedifferentiation and redifferentiation might have occurred. Since p48 was also expressed in acinar cells themselves (arrows in Fig. 6W,X), acinar cells might dedifferentiate and acquire an acinar progenitor character, which then redifferentiate into acinar cells. These cells renewed by themselves, which agreed with previous reports that preexisting acinar cells contribute to acinar cell regeneration (Jensen *et al.* 2005; Desai *et al.* 2007). Another possible interpretation is that ductal-to-acinar transdifferentiation occurred from Eppk1+ cells.

A partial pancreatectomy (Px) was also performed. It has been reported that a partial Px induce not only the

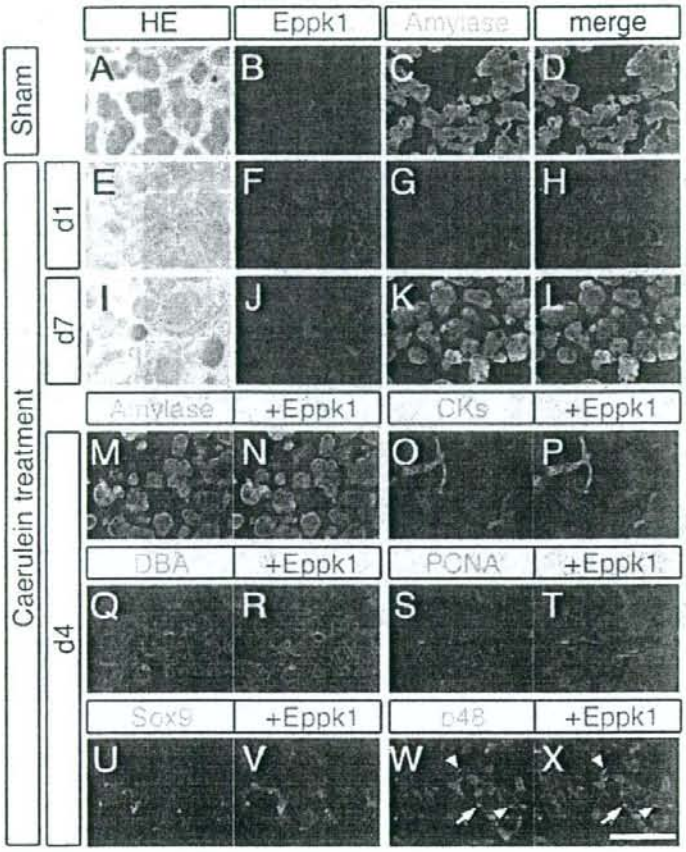

Figure 6 Eppk1 is expressed in the proliferating cells during acinar cell regeneration in caerulein-induced acute pancreatitis. (A–L) Histochemical analyses of the caerulein-treated pancreata. The images of H&E stainings of sham treated (A) and day one (E) or day 7 (I) after caerulein treatment are shown. Immunohistochemical analyses using anti-Eppk1 (B, F, J) and anti-Amylase (C, G, K) antibodies were also done. D, H and L are merged images. (M–X) Double immunostainings of Eppk1 with other markers in the pancreas on the 4th day after caerulein treatment are shown. Expressions of Amylase (M), Cytokeratins (O; CKs), DBA (Q), PCNA (S), Sox9 (U) and p48 (W) in Eppk1+ cells (N, P, R, T, V and X) were investigated. Arrowheads and arrows depict acinar progenitor cells or acinar cells. Scale bar, 100 μM (A–L), 50 μM (M–X).

proliferation of β cells (Dor *et al.* 2004), but also the regeneration, which recapitulated development of pancreas in the focal region. It was previously reported that small ductules were observed in the focal region (Bonner-Weir *et al.* 1993). These cells are called "ducts in foci", which are proposed to dedifferentiated/transdifferentiated from duct cells and differentiated into new lobes of pancreas, comprising both endocrine and exocrine tissues (Bonner-Weir *et al.* 1993). H&E staining of the pancreas on the next day after a partial Px revealed that eosin-stained acinar cells degeneration occurred and that leukocytes infiltrated into the focal region (Fig. 7A,B). On the 4th days after a Px, acinar cells degenerated and "ducts in foci" were observed (Fig. 7C,D, arrowheads in Fig. 7D). As previously reported (Bouwens *et al.* 1995), Cytokeratins were expressed in the "ducts in foci" (Fig. 7G), and Eppk1 was also observed in these cell (Fig. 7H). DBA reactivities were lost in these Eppk1+ cells (Fig. 7I,J) similar with the case in the caerulein-induced pancreatitis (Fig. 6Q,R). In some cells, Eppk1 expression overlapped with that of Amylase (arrowheads in Fig. 7E,F). There are also Eppk1+/Amylase- cells (arrows in Fig. 7E,F), thereby suggesting that some of the "ducts in foci" were dedifferentiated/transdifferentiated by acinoductal metaplasia (Lardon & Bouwens 2005). The number of Eppk1+ cells also increased by a factor of 4.96 (Supplementary Fig. S5 show low-magnification pictures; compare Supplementary Fig. S5E,F with Supplementary Fig. S5A,B), as in the caerulein-treated pancreas (Supplementary Fig. S5C,D). The ducts were Sox9+ (Fig. 7K,L) and PCNA+ (Fig. 7M,N), as seen in the ducts in the caerulein-treated pancreas (Fig. 6S–V). In Eppk1 KO mouse, Cytokeratins+ "ducts in foci" were observed (Fig. 7P) and PCNA was also

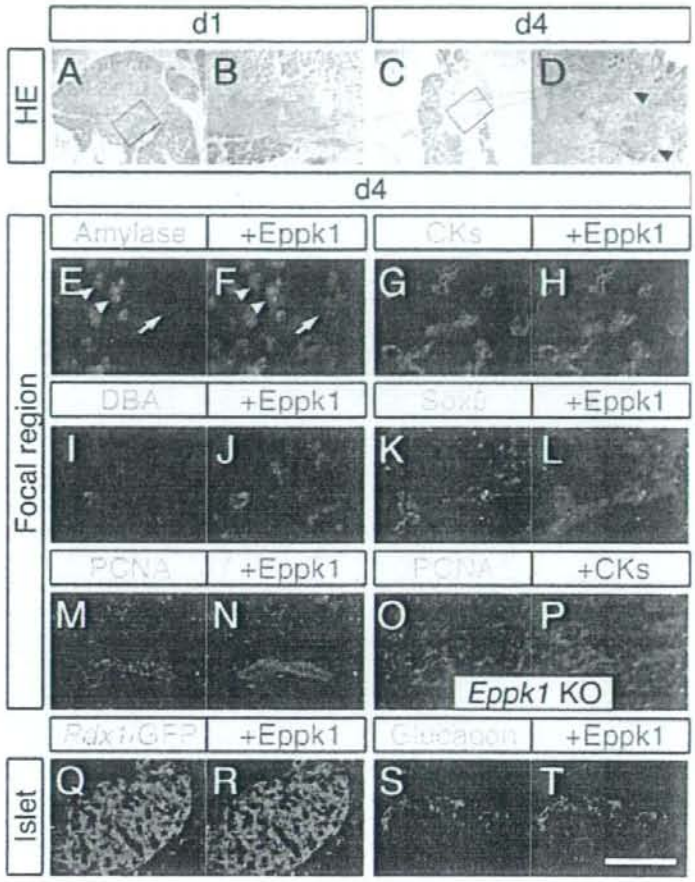

Figure 7 Eppk1 is expressed in the ducts in foci and α cells in the pancreas which has received a partial pancreatectomy. (A–D) The images of H&E stained sections of the pancreas one day (A, B) and 4 days (C, D) after a partial Px. B and D are magnified images in the focal region depicted by the squares in A and C, respectively. Arrowheads in D depict "ducts in foci". (E–T) Double immunostainings of Eppk1 and various markers in the focal region (E–P) and islet (Q–T) of the pancreas at day 4 after a partial Px was taken place. Arrows or arrowheads show Eppk1+/Amylase− or Eppk1+/Amylase + cells, respectively. Expressions of Amylase (E), Cytokeratins (G; CKs), DBA (I), Sox9 (K), PCNA (M, O), GFP of *Pdx1*/GFP mouse (Q) and Glucagon (S) in Eppk1-positive cells (F, H, J, L, N, R and T) were investigated. Eppk1 KO mouse was used in O and P with the counter staining done by using anti-panCK antibody (CKs). Scale bar, 1.2 mM (A, C), 400 μM (B, D), 100 μM (E–T).

observed (Fig. 7O), indicating that Eppk1 is not essential to form "ducts in foci" and that Eppk1 was not essential for the proliferating activity, either.

Eppk1 expression was observed in the islets in pancreata had a partial Px (Fig. 7Q,R). Further investigation revealed that the Eppk1+ cells were Glucagon-expressing α cells (Fig. 7S,T), which was similar to that seen in P0 islets (Fig. 3D–F).

Discussion

Eppk1 has been reported to be expressed in various organs by Northern blot analyses, including the pancreas (Fujiwara *et al.* 2001; Spazierer *et al.* 2003), but detailed expression patterns have not been examined. Studies of Eppk1 might reveal the molecular mechanism of signaling transduction underlying early pancreatic differentiation, and might shed lights on our future development of regenerative medicine for the cure of diabetes mellitus (Kume 2005a,b; Shiraki *et al.* 2005, 2008). In the present study, we focused on the expression patterns of Eppk1 in pancreas. We summarized the results in Fig. 8.

The Pdx1+ pancreatic progenitor cells have been shown to give rise to the cells of the endocrine, exocrine and duct lineages, that is, all lineages of cells existing in the adult pancreas (Jonsson *et al.* 1994; Offield *et al.* 1996; Gu *et al.* 2002). At E10.5, the pancreatic progenitor cells composed of cells with an almost complete overlap of Eppk1, Sox9 and Pdx1 expression (Fig. 1A–F; Fig. 8, E10.5 Pdx1+/Eppk1+/Sox9+ cells). Sox9 has been recently reported to maintain the multipotency of the pancreatic progenitor cell activity (Seymour *et al.* 2007).

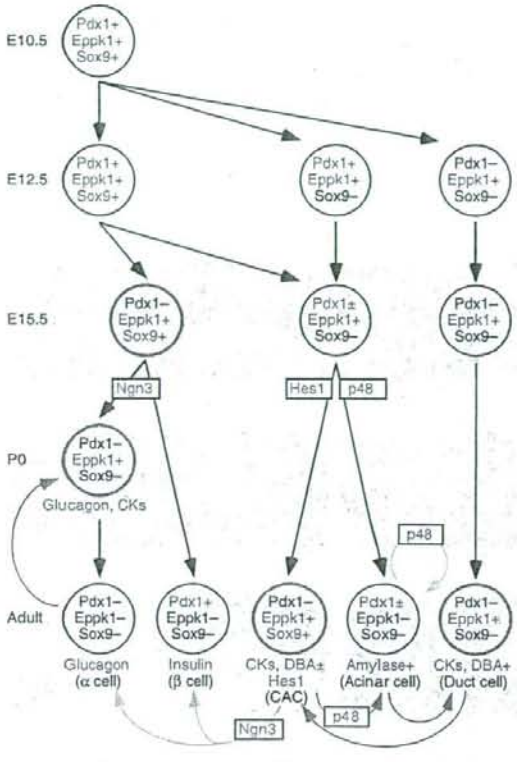

Figure 8 A schematic representation of Eppk1 expression. Expressions of Pdx1, Eppk and Sox9 are indicated in each cell lineage. Cells indicated by red and blue are those showing the same expression patterns of the three genes, respectively. Colored curved arrows show changes in gene expressions. See text in Discussion.

Then, in E12.5 pancreas Pdx1−/Sox9− cells appeared within the Eppk1+ cells (Fig. 1G–L). Gu *et al.* showed that pancreatic duct progenitors derived from multipotent pancreatic progenitor cells by E12.5, and differentiate into Pdx1− duct lineage cells (Gu *et al.* 2002). Thus, Eppk1+/Pdx1− cells (arrowheads in Fig. 1G–I) were possibly the progenitor cells of the ductal lineage (Fig. 8, E12.5 Pdx1−/Eppk1+/Sox9− cells). Since the expression of Pdx1 and Sox9 almost overlapped (Supplementary Fig. S2), Eppk1+/Sox9− cells (solid lines in Fig. 1J–L) and Eppk1+/Pdx1− cells (arrowheads in Fig. 1G–I) were possibly in the same population. Therefore, the Eppk1+/Sox9− cells were presumably to be Eppk1+/Pdx1−/Sox9− and also the progenitor of the ductal lineage. At this stage, Pdx1+/Sox9− cells began to emerge, which located at the edge of the pancreatic epithelium at this stage (arrowheads in Supplementary Fig. S2). These Pdx1+/Sox9− cells might be the progenitors of the exocrine cells (Fig. 8, E12.5 Pdx1+/Eppk1+/Sox9− cells). On the other hand, Sox9 is required for the expression of Ngn3 (Lynn *et al.* 2007), and for the endocrine cell differentiation to be switched on (Gradwohl *et al.* 2000; Jensen *et al.* 2000; Schwitzgebel *et al.* 2000; Gu *et al.* 2002). Pdx1+/Eppk1+/Sox9+ population correspond to multipotent progenitor cells (Fig. 8, E12.5 Pdx1+/Eppk1+/Sox9+ cells).

In the pancreas of E15.5 embryo, the expression of Eppk1 was not detected in Pdx1+ cells (Fig. 2A–C), most of which expressed insulin (Supplementary Fig. S3), suggesting that these cells are differentiating toward a β cell fate. Eppk1+/Sox9+ cells form a "central duct-like structure", in which the expression of Ngn3 was observed (Fig. 2D–I), indicating that Eppk1 marks the endocrine progenitor at this stage (Fig. 8, E15.5 Pdx1−/Eppk1+/Sox9+ cells; red circle). On the other hand, the exocrine cell progenitors form acini at this stage (Jensen 2004), in which strong Eppk1 and weak Pdx1 expression was observed (Fig. 2J–O; Fig. 8, E15.5 Pdx1±/Eppk1+/Sox9− cells), suggesting that Eppk1 serves also as an exocrine progenitor cell marker. The expressions of Hes1 in the center position and p48 in the outer side were observed in the forming acini (Fig. 2J–O). p48 is a subunit of Ptf1α, which is essential for differentiation of pancreatic exocrine cells (Krapp *et al.* 1996, 1998). Hes1 is a Notch signaling related transcriptional factor, which sustains immaturity of the cells (Kageyama *et al.* 2005). Esni *et al.* reported that p48+/Hes1+ double positive common progenitor cells diverged into p48+/Hes− exocrine precursor cells, and p48−/Hes1+ Notch-regulated progenitor cells (Esni *et al.* 2004).

In the adult pancreas, Eppk1 was expressed in duct cells and in CACs, which were Sox9+/Hes1+ cells (Fig. 4). Thus, it was suggested that p48+/Hes1+ common progenitor cells differentiated into the pancreatic exocrine cells (Fig. 8, Pdx1±/Eppk1−/Sox9−) and CACs (Fig. 8, Pdx1−/Eppk1+/Sox9+, red circle), which was possibly Notch-regulated progenitor cells. Among the hormone expressing cells in postnatal pancreas, Eppk1 was detected only in α cells in perinatal pancreas (Fig. 8, P0 Pdx1−/Eppk1+/Sox9−), which were also Cytokeratin+ (Fig. 3). The expression of Eppk1 and Cytokeratins disappeared in the adult (Fig. 4A–C; Fig. 8, α cells Pdx1−/Eppk1−/Sox9−).

It is hypothesized that some cancers represent an aberrant recapitulation of normal development (Hezel *et al.* 2006). It is further deducted that some cancers can be originated from adult tissue stem cells. The activations of PI3K (Stanger *et al.* 2005), Notch and TGFα signalings

(Miyamoto *et al.* 2003) in CACs gave rise to PanIN, which has been shown to be a precursor lesion of PDAC (Hezel *et al.* 2006). Eppk1 was also expressed in the early stage of PanIN cells (Fig. 5A–J). Hes1, a transcription factor downstream of Notch signaling, was expressed in CACs (Fig. 4P–R) (Miyamoto *et al.* 2003), and Eppk1 was reported to bind to EGF receptor (Blagoev *et al.* 2003). However, the expression of Eppk1 in PanIN cells gradually decreased, similarly with that of Cytokeratins (Fig. 5Q–T). The relation between Eppk1 and EGF were not clear at the moment.

Next we observed the expression patterns of Eppk1 in regenerating pancreas. Based on the findings of genetic tracing experiments, it is reported that β cells (Dor *et al.* 2004) and acinar cells (Desai *et al.* 2007) normally renew themselves slowly. However, when injured, immediate repair is taken place in the pancreas of rodents. Acinar cell regeneration in an acute pancreatitis model (Gasslander *et al.* 1992; Jensen *et al.* 2005) by injection of caerulein and islet regeneration in a partial Px model (Bonner-Weir *et al.* 1993) are well-known. Here, in both caerulein treatment and a partial Px, Eppk1+/Cytokeratins+ cells appeared among acinar cells, which were possibly formed by acinoductal metaplasia (a brown curved arrow in Fig. 8) (Lardon & Bouwens 2005) or dedifferentiated/transdifferentiated from duct cells, in which PCNA and Sox9 were expressed later (Figs 6 and 7; a red curved arrow in Fig. 8). Recently, it was shown that new endocrine cells were differentiated from duct cells in a partial duct ligated pancreas (Xu *et al.* 2008). In the report, Ngn3+ cells appeared from duct cells and differentiated into α and β cells. Since the gene expressions and the morphologies of the duct cells of injured pancreata and "central duct-like structure" in E15.5 pancreas were similar (compare Figs 2, 6 and 7; red circles in Fig. 8), the characteristics of the cells may also be similar. Ngn3 was reported to be expressed in Sox9+ cells (Lynn *et al.* 2007), which correspond to the Pdx1−/Eppk1+/Sox9+ cells in the "central duct-like structure" (Fig. 8 E15.5 red circle). According to our above hypothesis, the Ngn3+ cells derived from the duct cells of the partial duct ligated pancreas (Xu *et al.* 2008) are similar with Pdx1−/Eppk1+/Sox9+ CACs, which might give rise to endocrine cells upon duct certain injury (a green arrow in Fig. 8) (Lynn *et al.* 2007). Furthermore, we found p48 to be expressed in the Eppk1+ cells (arrowheads in Fig. 6W,X), indicating that Eppk1 was a marker of the progenitor cells of acinar cell regeneration. p48 was also detected in the acinar cells themselves, indicating that during regeneration of acinar cells, either dedifferentiation from acinar cells (a brown arrow in Fig. 8), differentiation of progenitor cells (a purple arrow in Fig. 8) or simply proliferation of existing acinar cells (a lime green line in Fig. 8) is supposed to occur. Cytokeratins+"duct in foci" in *Eppk1* KO mouse were also PCNA+ (Fig. 7O,P), indicating that Eppk1 was not essential for maintaining stem cell activity. In islets, Eppk1 was expressed in α cells of perinatal pancreas (Fig. 3D–F), which gradually disappeared toward the adult (Fig. 4A–C). In the perinatal pancreas, islets were located near by the duct cells, which were also Eppk1+ (Fig. 4I–L; blue circles in Fig. 8). α cells and duct cells may have similar characteristics and some interactions at this stage. Islets at this stage often were "dump-bell" shaped (Supplementary Fig. S6A), though they were usually spherical in the adult (Supplementary Fig. S6B), as a result of fission (Seymour *et al.* 2004). The expression of Eppk1 in α cells was observed again in the islets of pancreas that had a partial Px (Fig. 7S,T; a blue arrow in Fig. 8), which also showed "dump-bell" shape (Supplementary Fig. S6C). Eppk1 may be involved in the motility of islets.

In summary, we examined the expression patterns of Eppk1 in pancreas and showed that Eppk1 serves as an excellent marker to analyze the cell lineage of pancreas.

Experimental procedures

Animals and pancreas regeneration models

A transgenic mouse line *Pdx1*/GFP (Gu *et al.* 2004) was a gift from Dr Melton of Harvard University. Wild-type ICR mice were obtained from SLC (Kanagawa, Japan). The date of conception was established by the presence of a vaginal plug and recorded as E0.5. 8-week-old mice were used as adults. Caerulein treatment was carried out as previously described (Jensen *et al.* 2005). A Px was carried out as previously described (Bonner-Weir *et al.* 1993).

Antibodies

Two kinds of rabbit anti-Eppk1antibodies were used: one is described previously (Fujiwara *et al.* 2001) and another is a gift from Dr G. Wiche of University of Vienna (Spazierer *et al.* 2003). Guinea pig anti-Hes1 antibody was a gift from Dr R. Kageyama (Kyoto University) (Hatakeyama *et al.* 2006). Rabbit anti-p48 antibody was kindly provided by Dr H. Edlund (Li & Edlund 2001). Mouse anti-Ngn3 (Cat #F25A1B3) (Zahn *et al.* 2004) antibody was obtained from Developmental Studies Hybridoma Bank. The other primary antibodies used were mouse anti-Insulin (Cat #I-2018, Sigma, St. Louis, MO), mouse anti-Glucagon (Cat #G-2654, Sigma), mouse anti-GFP (Cat #11814460001, Roche, Indianapolis, IN), mouse ant-pan Cytokeratin (Cat #ab11213, Abcam, Cambridge, UK), mouse anti-PCNA (Cat #NA03, Oncogene Research Products, Boston, MA), rabbit anti-Pdx1 (Cat #KAL-KR059, Trans Genic Inc., Kumamoto, Japan), rabbit anti-human Glucagon (Cat #A0565, Dako Cytomation, Glostrup, Denmark), goat anti-Amylase (Cat #sc-12821, Santa Cruz Biotechnology Inc., Santa Cruz, CA) and goat anti-Sox9

(Cat #sc-17340, Santa Cruz Biotechnology Inc.) antibodies. Fluorescein isothiocyanate conjugated DBA (*Dolichos biflorus* agglutinin, Vector Laboratories Inc., Burlingame, CA) was also used.

Immunological analyses

Immunohistochemical analyses of the frozen sections and paraffin sections were performed as described previously (Yoshida *et al.* 2003). First, sections were boiled in Target Retrieval Solution (Dako Cytomation) for 10 min at 105 °C for antigen retrieval. Bound first antibodies were visualized with Alexa 488 or Alexa 568 labeled appropriate secondary antibodies (Invitrogen, Carlsbad, CA). Double immunostaining using rabbit anti-Eppk1 and rabbit anti-p48 antibodies was performed as follows: First anti-p48 antibody was bound to a frozen section and visualized by Alexa 488-conjugated anti-rabbit IgG antibody. Then, anti-Eppk1 antibody, which was biotinylated by Biotin Labeling Kit-NH2 (Dojindo Laboratories, Kumamoto, Japan) according to the procedure recommended by the manufacturer, was bound after blocking using non immunized rabbit serum. The expression pattern of Eppk1 was visualized by streptavidin-conjugated Alexa 588. The nuclei were counterstained using DAPI (Roche). Optical sections were viewed using a scanning laser confocal imaging system (TCSSP2 AOBS, Leica Microsystems, Wetzler, Germany). Non confocal images were acquired using an Olympus IX-71 microscope (Olympus Optical, Tokyo, Japan) equipped with a Nikon digital sight DS-5M (Tokyo, Japan). Images were processed using Adobe Photoshop 7.0 (Adobe Systems, San Jose, CA). The numbers of stained cells in Supplementary Fig. S5 were quantified by analyzing the areas of Eppk1+ staining images using Lumina Vision program (Mitani Corporation, Fukui, Japan).

Acknowledgements

We are grateful for Dr G. Wiche (University of Vienna), Dr H. Edlund (University of Umea), Dr R. Kageyama (Kyoto University) and Dr J. Hatakeyama (Kumamoto University) for providing antibodies. We also thank Dr D. Melton (Harvard University) and Dr G. Gu (Vanderbilt University) for providing *Pdx1*/GFP mice. This work was supported by grants (No. 17045026 and 16027239 to S.K. and No. 17790611 to T.Y.), from the Ministry of Education, Culture, Sports, Science and Technology (MEXT) of Japan, by a grant (to S.K.) from the Project for Realization of Regenerative Medicine from MEXT, and a Twenty-first Century Center-of-Excellence (COE) grant, and a Global COE grant from MEXT. T.Y. and N.S. are research associates of the Twenty-first COE. N.S. is a research associate of the Global COE program. This work was also supported in part by a grant (to S.K.) from the New Energy and Industrial Technology Development Organization.

References

Blagoev, B., Kratchmarova, I., Ong, S.E., Nielsen, M., Foster, L.J. & Mann, M. (2003) A proteomics strategy to elucidate functional protein-protein interactions applied to EGF signaling. *Nat. Biotechnol.* **21**, 315–318.

Bonner-Weir, S., Baxter, L.A., Schuppin, G.T. & Smith, F.E. (1993) A second pathway for regeneration of adult exocrine and endocrine pancreas. A possible recapitulation of embryonic development. *Diabetes* **42**, 1715–1720.

Bouwens, L., Wang, R.N., De Blay, E., Pipeleers, D.G. & Kloppel, G. (1994) Cytokeratins as markers of ductal cell differentiation and islet neogenesis in the neonatal rat pancreas. *Diabetes* **43**, 1279–1283.

Bouwens, L., Braet, F. & Heimberg, H. (1995) Identification of rat pancreatic duct cells by their expression of cytokeratins 7, 19, and 20 *in vivo* and after isolation and culture. *J. Histochem. Cytochem.* **43**, 245–253.

Desai, B.M., Oliver-Krasinski, J., De Leon, D.D., Farzad, C., Hong, N., Leach, S.D. & Stoffers, D.A. (2007) Preexisting pancreatic acinar cells contribute to acinar cell, but not islet β cell, regeneration. *J. Clin. Invest.* **117**, 971–977.

Dor, Y., Brown, J., Martinez, O.I. & Melton, D.A. (2004) Adult pancreatic β-cells are formed by self-duplication rather than stem-cell differentiation. *Nature* **429**, 41–46.

Esni, F., Ghosh, B., Biankin, A.V., Lin, J.W., Albert, M.A., Yu, X., MacDonald, R.J., Civin, C.I., Real, F.X., Pack, M.A., Ball, D.W. & Leach, S.D. (2004) Notch inhibits Ptf1 function and acinar cell differentiation in developing mouse and zebrafish pancreas. *Development* **131**, 4213–4224.

Fujiwara, S., Takeo, N., Otani, Y., Parry, D.A., Kunimatsu, M., Lu, R., Sasaki, M., Matsuo, N., Khaleduzzaman, M. & Yoshioka, H. (2001) Epiplakin, a novel member of the Plakin family originally identified as a 450-kDa human epidermal autoantigen. Structure and tissue localization. *J. Biol. Chem.* **276**, 13340–13347.

Gallicano, G.I., Kouklis, P., Bauer, C., Yin, M., Vasioukhin, V., Degenstein, L. & Fuchs, E. (1998) Desmoplakin is required early in development for assembly of desmosomes and cytoskeletal linkage. *J. Cell Biol.* **143**, 2009–2022.

Gasslander, T., Ihse, I. & Smeds, S. (1992) The importance of the centroacinar region in cerulein-induced mouse pancreatic growth. *Scand. J. Gastroenterol* **27**, 564–570.

Goto, M., Sumiyoshi, H., Sakai, T., Fassler, R., Ohashi, S., Adachi, E., Yoshioka, H. & Fujiwara, S. (2006) Elimination of epiplakin by gene targeting results in acceleration of keratinocyte migration in mice. *Mol. Cell. Biol.* **26**, 548–558.

Gradwohl, G., Dierich, A., LeMeur, M. & Guillemot, F. (2000) neurogenin3 is required for the development of the four endocrine cell lineages of the pancreas. *Proc. Natl. Acad. Sci. USA* **97**, 1607–1611.

Gu, G., Dubauskaite, J. & Melton, D.A. (2002) Direct evidence for the pancreatic lineage: NGN3+ cells are islet progenitors and are distinct from duct progenitors. *Development* **129**, 2447–2457.

Gu, G., Wells, J.M., Dombkowski, D., Preffer, F., Aronow, B. & Melton, D.A. (2004) Global expression analysis of gene regulatory pathways during endocrine pancreatic development. *Development* **131**, 165–179.

Guo, L., Degenstein, L., Dowling, J., Yu, Q.C., Wollmann, R., Perman, B. & Fuchs, E. (1995) Gene targeting of BPAG1: abnormalities in mechanical strength and cell migration in stratified epithelia and neurologic degeneration. *Cell* **81**, 233–243.

Hatakeyama, J., Sakamoto, S. & Kageyama, R. (2006) Hes1 and Hes5 regulate the development of the cranial and spinal nerve systems. *Dev. Neurosci.* **28**, 92–101.

Hezel, A.F., Kimmelman, A.C., Stanger, B.Z., Bardeesy, N. & Depinho, R.A. (2006) Genetics and biology of pancreatic ductal adenocarcinoma. *Genes Dev.* **20**, 1218–1249.

Jang, S.I., Kalinin, A., Takahashi, K., Marekov, L.N. & Steinert, P.M. (2005) Characterization of human epiplakin: RNAi-mediated epiplakin depletion leads to the disruption of keratin and vimentin IF networks. *J. Cell Sci.* **118**, 781–793.

Jensen, J. (2004) Gene regulatory factors in pancreatic development. *Dev. Dyn.* **229**, 176–200.

Jensen, J., Heller, R.S., Funder-Nielsen, T., Pedersen, E.E., Lindsell, C., Weinmaster, G., Madsen, O.D. & Serup, P. (2000) Independent development of pancreatic α- and β-cells from neurogenin3-expressing precursors: a role for the notch pathway in repression of premature differentiation. *Diabetes* **49**, 163–176.

Jensen, J.N., Cameron, E., Garay, M.V., Starkey, T.W., Gianani, R. & Jensen, J. (2005) Recapitulation of elements of embryonic development in adult mouse pancreatic regeneration. *Gastroenterology* **128**, 728–741.

Jonsson, J., Carlsson, L., Edlund, T. & Edlund, H. (1994) Insulin-promoter-factor 1 is required for pancreas development in mice. *Nature* **371**, 606–609.

Kageyama, R., Ohtsuka, T., Hatakeyama, J. & Ohsawa, R. (2005) Roles of bHLH genes in neural stem cell differentiation. *Exp. Cell Res.* **306**, 343–348.

Krapp, A., Knofler, M., Frutiger, S., Hughes, G.J., Hagenbuchle, O. & Wellauer, P.K. (1996) The p48 DNA-binding subunit of transcription factor PTF1 is a new exocrine pancreas-specific basic helix–loop–helix protein. *EMBO J.* **15**, 4317–4329.

Krapp, A., Knofler, M., Ledermann, B., Burki, K., Berney, C., Zoerkler, N., Hagenbuchle, O. & Wellauer, P.K. (1998) The bHLH protein PTF1-p48 is essential for the formation of the exocrine and the correct spatial organization of the endocrine pancreas. *Genes Dev.* **12**, 3752–3763.

Kume, S. (2005a) The molecular basis and prospects in pancreatic development. *Dev. Growth Differ.* **47**, 367–374.

Kume, S. (2005b) Stem-cell-based approaches for regenerative medicine. *Dev. Growth Differ.* **47**, 393–402.

Lardon, J. & Bouwens, L. (2005) Metaplasia in the pancreas. *Differentiation* **73**, 278–286.

Li, H. & Edlund, H. (2001) Persistent expression of Hlxb9 in the pancreatic epithelium impairs pancreatic development. *Dev. Biol.* **240**, 247–253.

Lynn, F.C., Smith, S.B., Wilson, M.E., Yang, K.Y., Nekrep, N. & German, M.S. (2007) Sox9 coordinates a transcriptional network in pancreatic progenitor cells. *Proc. Natl. Acad. Sci. USA* **104**, 10500–10505.

Miettinen, P.J., Huotari, M., Koivisto, T., Ustinov, J., Palgi, J., Rasilainen, S., Lehtonen, E., Keski-Oja, J. & Otonkoski, T. (2000) Impaired migration and delayed differentiation of pancreatic islet cells in mice lacking EGF-receptors. *Development* **127**, 2617–2627.

Miyamoto, Y., Maitra, A., Ghosh, B., Zechner, U., Argani, P., Iacobuzio-Donahue, C.A., Sriuranpong, V., Iso, T., Meszoely, I.M., Wolfe, M.S., Hruban, R.H., Ball, D.W., Schmid, R.M. & Leach, S.D. (2003) Notch mediates TGF α-induced changes in epithelial differentiation during pancreatic tumorigenesis. *Cancer Cell* **3**, 565–576.

Offield, M.F., Jetton, T.L., Labosky, P.A., Ray, M., Stein, R.W., Magnuson, M.A., Hogan, B.L. & Wright, C.V. (1996) PDX-1 is required for pancreatic outgrowth and differentiation of the rostral duodenum. *Development* **122**, 983–995.

Schwitzgebel, V.M., Scheel, D.W., Conners, J.R., Kalamaras, J., Lee, J.E., Anderson, D.J., Sussel, L., Johnson, J.D. & German, M.S. (2000) Expression of neurogenin3 reveals an islet cell precursor population in the pancreas. *Development* **127**, 3533–3542.

Seymour, P.A., Bennett, W.R. & Slack, J.M. (2004) Fission of pancreatic islets during postnatal growth of the mouse. *J. Anat.* **204**, 103–116.

Seymour, P.A., Freude, K.K., Tran, M.N., Mayes, E.E., Jensen, J., Kist, R., Scherer, G. & Sander, M. (2007) SOX9 is required for maintenance of the pancreatic progenitor cell pool. *Proc. Natl. Acad. Sci. USA* **104**, 1865–1870.

Shiraki, N., Lai, C.J., Hishikari, Y. & Kume, S. (2005) TGF-β signaling potentiates differentiation of embryonic stem cells to Pdx-1 expressing endodermal cells. *Genes Cells* **10**, 503–516.

Shiraki, N., Yoshida, T., Araki, K., Umezawa, A., Higuchi, Y., Goto, H., Kume, K. & Kume, S. (2008) Guided differentiation of ES cells into Pdx1-expressing regional specific definitive endoderm. *Stem Cells* **26**.

Slack, J.M. (1995) Developmental biology of the pancreas. *Development* **121**, 1569–1580.

Smith, F.J., Eady, R.A., Leigh, I.M. *et al.* (1996) Plectin deficiency results in muscular dystrophy with epidermolysis bullosa. *Nat. Genet.* **13**, 450–457.

Sonnenberg, A. & Liem, R.K. (2007) Plakins in development and disease. *Exp. Cell Res.* **313**, 2189–2203.

Spazierer, D., Fuchs, P., Proll, V., Janda, L., Oehler, S., Fischer, I., Hauptmann, R. & Wiche, G. (2003) Epiplakin gene analysis in mouse reveals a single exon encoding a 725-kDa protein with expression restricted to epithelial tissues. *J. Biol. Chem.* **278**, 31657–31666.

Spazierer, D., Fuchs, P., Reipert, S., Fischer, I., Schmuth, M., Lassmann, H. & Wiche, G. (2006) Epiplakin is dispensable for skin barrier function and for integrity of keratin network cytoarchitecture in simple and stratified epithelia. *Mol. Cell. Biol.* **26**, 559–568.

Stanger, B.Z., Stiles, B., Lauwers, G.Y., Bardeesy, N., Mendoza, M., Wang, Y., Greenwood, A., Cheng, K.H., McLaughlin, M., Brown, D., Depinho, R.A., Wu, H., Melton, D.A. & Dor, Y. (2005) Pten constrains centroacinar cell expansion and malignant transformation in the pancreas. *Cancer Cell* **8**, 185–195.

Xu, X., D'Hoker, J., Stange, G., Bonne, S., De Leu, N., Xiao, X., Van de Casteele, M., Mellitzer, G., Ling, Z., Pipeleers, D., Bouwens, L., Scharfmann, R., Gradwohl, G. & Heimberg, H. (2008) β cells can be generated from endogenous progenitors in injured adult mouse pancreas. *Cell* **132**, 197–207.

Yoshida, T., Tokunaga, A., Nakao, K. & Okano, H. (2003) Distinct expression patterns of splicing isoforms of mNumb in the endocrine lineage of developing pancreas. *Differentiation* **71**, 486–495.

Zahn, S., Hecksher-Sorensen, J., Pedersen, I.L., Serup, P. & Madsen, O. (2004) Generation of monoclonal antibodies against mouse neurogenin3: a new immunocytochemical tool to study the pancreatic endocrine progenitor cell. *Hybrid Hybridomics* **23**, 385–388.

Received: 27 November 2007
Accepted: 30 March 2008

Supplementary material

The following supplementary material is available for this article:

Figure S1 The expressions of GFP are well-concerned with those of Pdx1 in all of the developmental stages of *Pdx1*/GFP mouse.

Figure S2 Sox9 is not expressed in all of the Pdx1-positive cells of E12.5 pancreas.

Figure S3 Almost all Pdx1-positive cells are β cells in E15.5 pancreas.

Figure S4 Cytokeratins are expressed in α cells of P0 pancreas.

Figure S5 Low magnification pictures of Eppk1+ cells after injury.

Figure S6 Morphologies of the islets of P0, adult and adult Px pancreas.

This material is available as part of the online article from:
http://www.blackwell-synergy.com/doi/abs/10.1365-2443.2008.01196.x
(This link will take you to the article abstract).

Please note: Blackwell Publishing are not responsible for the content or functionality of any supplementary materials supplied by the authors. Any queries (other than missing material) should be directed to the corresponding author for the article.

J Hepatobiliary Pancreat Surg (2009) 16:49–55
DOI 10.1007/s00534-008-0004-3

ORIGINAL ARTICLE

Prospective randomized controlled study of gastric emptying assessed by ^{13}C-acetate breath test after pylorus-preserving pancreaticoduodenectomy: comparison between antecolic and vertical retrocolic duodenojejunostomy

Kazuo Chijiiwa · Naoya Imamura · Jiro Ohuchida · Masahide Hiyoshi · Motoaki Nagano · Kazuhiro Otani · Masahiro Kai · Kazuhiro Kondo

Received: 16 November 2007 / Accepted: 16 January 2008 / Published online: 16 December 2008

Abstract
Background/Purpose To examine whether vertical retrocolic duodenojejunostomy is superior to antecolic duodenojejunostomy with respect to gastric emptying in a prospective, randomized, controlled study of patients undergoing pylorus-preserving pancreaticoduodenectomy (PpPD).
Methods Thirty-five patients undergoing PpPD between March 2005 and July 2007 were enrolled in the study. All provided informed consent. During PpPD, the patients were randomly assigned to either the antecolic (antecolic group, $n = 17$) or vertical retrocolic route (vertical retrocolic group, $n = 18$) just before the reconstruction. Each patient ingested ^{13}C-acetate in a liquid meal before surgery and on postoperative day (POD) 30. Gastric emptying variables (Tmax, T1/2) were determined and compared between groups.
Results Clinical delayed gastric emptying, defined as an inability of patients to take in an appropriate amount of solid food orally by POD 14, was found in 1 of 17 patients (6%) in the antecolic group and in 4 of 18 patients (22%) in the vertical retrocolic group, but the difference was not significant ($P = 0.34$). Tmax and T1/2 on POD 30 were prolonged in both groups in comparison to preoperative levels, but no significant difference was found between the two groups. Follow-up examinations revealed that gastric emptying had recovered to the preoperative level by POD 30 in approximately 80% of the patients, regardless of the reconstruction route.
Conclusions Vertical retrocolic duodenojejunostomy does not seem to offer an advantage with respect to gastric emptying.

Keywords Gastric emptying · Pylorus-preserving pancreaticoduodenectomy · Antecolic duodenojejunostomy · Vertical retrocolic duodenojejunostomy

K. Chijiiwa · N. Imamura · J. Ohuchida · M. Hiyoshi · M. Nagano · K. Otani · M. Kai · K. Kondo
Department of Surgical Oncology and Regulation of Organ Function, Miyazaki University School of Medicine, Kihara 5200, Kiyotake, Miyazaki, Japan

K. Chijiiwa (✉)
Department of Surgery, Miyazaki University School of Medicine, Kihara 5200, Kiyotake, Miyazaki, Japan
e-mail: kazuochi@med.miyazaki-u.ac.jp

Introduction

Pylorus-preserving pancreaticoduodenectomy (PpPD) is generally accepted as a standard operation for periampullary lesions. PpPD, in comparison to classic pancreaticoduodenectomy with hemigastrectomy, is reported to improve quality of life, nutritional status and weight gain without any difference in operative morbidity and mortality or in postoperative survival [1–4].

Delayed gastric emptying (DGE), however, is reported to be the most common and frustrating complication after PpPD. Despite the lack of a certain definition for DGE, the reported incidence varies from 20 to 60% [5–13]. DGE results in a prolonged hospital stay, which adds to hospital costs. Although DGE itself is not a fatal complication, minimizing DGE is important in patients undergoing PpPD.

Two reconstruction routes are used for duodenojejunostomy, the antecolic route and the retrocolic route. The reported incidence of DGE is >30% for the retrocolic route [12, 14, 15], whereas that for the antecolic route is <15%